AWARD NUMBER: W81XWH-18-1-0497

TITLE: Does TBI Affect mtDNA Heteroplasmy?

PRINCIPAL INVESTIGATOR: Janna Harris

CONTRACTING ORGANIZATION: University of Kansas, Medical Center Research Institute, Inc., Shawnee Mission, KS

REPORT DATE: December 2022

TYPE OF REPORT: Final

PREPARED FOR: U.S. Army Medical Research and Development Command
Fort Detrick, Maryland 21702-5012

REPORT DOCUMENTATION PAGE

Form Approved
OMB No. 0704-0188

1. REPORT DATE	2. REPORT TYPE	3. DATES COVERED
December 2022	Final	15Aug2018-14Aug2022

4. TITLE AND SUBTITLE

Does TBI Affect mtDNA Heteroplasmy?

5a. CONTRACT NUMBER
W81XWH-18-1-0497

5b. GRANT NUMBER

5c. PROGRAM ELEMENT NUMBER

6. AUTHOR(S)

Janna L Harris, PhD

E-Mail:

5d. PROJECT NUMBER

5e. TASK NUMBER

5f. WORK UNIT NUMBER

7. PERFORMING ORGANIZATION NAME(S) AND ADDRESS(ES)

UNIVERSITY OF KANSAS
MEDICAL CENTER RESE KUMC RESEARCH INTITUTE
4330 SHAWNEE MISSION PKWY
SHAWNEE MISSION KS 66205-2522

8. PERFORMING ORGANIZATION REPORT NUMBER

9. SPONSORING / MONITORING AGENCY NAME(S) AND ADDRESS(ES)

U.S. Army Medical Research and Development Command
Fort Detrick, Maryland 21702-5012

10. SPONSOR/MONITOR'S ACRONYM(S)

11. SPONSOR/MONITOR'S REPORT NUMBER(S)

12. DISTRIBUTION / AVAILABILITY STATEMENT

Approved for Public Release; Distribution Unlimited

13. SUPPLEMENTARY NOTES

14. ABSTRACT

This collaborative project sought to better understand the long-term consequences of traumatic brain injury (TBI) as they pertain to Alzheimer's disease (AD). To accomplish this, we conducted a series of experiments to explore connections between TBI, brain aging, and mitochondrial DNA (mtDNA) mutations. Our central hypothesis was that TBI accelerates the age-related accumulation of mtDNA microheteroplasmic mutations, and that this can explain the recognized association between TBI and AD. To test this, we exposed young adult mice to a TBI or sham injury and let the mice age.
Age-related tissue shrinkage made the quantification of ultra-low frequency heteroplasmic mutations in mouse hippocampus samples too unreliable, so we pursued an alternate approach by quantifying mitochondrial DNA copy number (mtDNAcn), another marker of aging-related mitochondrial change. We found an enhanced aging-related mtDNAcn increase in brain-injured mice compared to controls, suggesting that the amount of compensation required to preserve mitochondrial function late in life may be greater after a brain injury. TBI may, therefore, increase AD risk by affecting the biology or trajectory of aging-related mitochondrial adaptation.

15. SUBJECT TERMS
None listed.

16. SECURITY CLASSIFICATION OF:			17. LIMITATION OF ABSTRACT	18. NUMBER OF PAGES	19a. NAME OF RESPONSIBLE PERSON
a. REPORT	b. ABSTRACT	c. THIS PAGE			USAMRDC
Unclassified	Unclassified	Unclassified	Unclassified	53	19b. TELEPHONE NUMBER *(include area code)*

TABLE OF CONTENTS

1. Introduction

This collaborative project has sought to better understand the long-term consequences of traumatic brain injury (TBI) as they pertain to Alzheimer's disease (AD). To accomplish this, conducted a series of experiments to explore connections between TBI, brain aging, and mitochondrial DNA (mtDNA) mutations. Our central hypothesis is that TBI accelerates the age-related accumulation of mtDNA microheteroplasmic mutations, and that this can explain the recognized association between TBI and AD. To test this, we exposed young adult mice to a TBI or sham intervention and let the mice age. In Aim 1, we examined whether the TBI sustained during young adulthood accelerates the age-related accumulation of mtDNA heteroplasmy. In Aim 2, we characterized these aging, brain-injured mice through behavioral testing, magnetic resonance imaging and spectroscopy, and measurements of mitochondrial enzyme activity, and we correlated mtDNA heteroplasmy with these endpoints. In Aim 3, we administered CCI to young adult rTg4510 mice (which accumulate neurofibrillary tangles), aged the mice, quantified mtDNA heteroplasmy and neurofibrillary tangle burden, and tested relationships between these two parameters.

Due to age-related shrinkage of the hippocampi we were unable to reliably quantify ultra-low frequency heteroplasmic mutations in our post-aging and transgenic mouse brain samples via established methods. After two years of efforts by our team to develop novel methods to overcome this challenge, the co-PIs decided to pursue an alternative approach by quantifying mitochondrial DNA copy number (mtDNAcn), an alternative marker of aging-related mitochondrial change. As detailed in this report and in our recently submitted manuscript (See Appendix A), we found an enhanced aging-related mtDNAcn increase in brain-injured mice compared to controls, suggesting that the amount of compensation required to preserve mitochondrial function late in life may be greater after a brain injury. TBI may, therefore, increase AD risk by affecting the biology of aging-related mitochondrial adaptation.

2. Keywords

Traumatic brain injury
Alzheimer's disease
Aging
Mitochondrial DNA
Mutations
Functional impairment
Memory
Magnetic resonance imaging
Tau pathology

3. Accomplishments

The major goals of the project were:

Specific Aim 1: Test whether a young adulthood CCI injury accelerates the age-dependent accumulation of mtDNA.

Specific Aim 2: Test whether brain mtDNA heteroplasmy in aged mice subjected to young adulthood CCI injury relates to behavioral function, brain metabolism, and brain structure.

Specific Aim 3: Test whether neurofibrillary tangle burden in aged rTg4510 mice subjected to young adulthood CCI injury relates to mtDNA mutations.

Accomplishments under these goals:

Specific Aim 1: we have completed all of the following tasks described in the SOW.

- Local IACUC Review/Approval

- ACURO Review/Approval

- Acquire mice; acquisition will be staggered (Total of 82 C57Bl/6 mice)

- Administer CCI

- Sacrifice mice and collect hippocampal DNA 1 month following CCI

- Age the mice

- Sacrifice mice/collect hippocampal DNA 15 months following CCI

- Analyze mitochondrial DNA copy number in mouse hippocampi*

We found that TBI enhance the aging-associated increase in mtDNA copy number. See results in **Appendix A, Figures 5, 6.**

**Note:* as described above, measuring mtDNAcn is an alternative approach we used to assess aging-related changes in brain mitochondria. We elected to move forward with this alternative approach after our extensive efforts to adapt existing methods for sequencing low-frequency mtDNA heteroplasmy failed to generate reliable results in the shrunken hippocampal samples collected from the injured/aged and transgenic mice in this study.

- Milestone Achieved: Manuscript prepared and submitted.

Specific Aim 2: we have completed all of the following tasks described in the SOW.

- Local IACUC Review/Approval

- ACURO Review/Approval

- Acquire mice (same 82 mice as Specific Aim 1)

- Administer CCI

- Assess cognitive and motor function immediately before CCI, immediately following CCI, 1 month after CCI, and 15 months after CCI

Results show that mice were impaired on the full battery of cognitive and motor tests acutely after CCI, and that functional impairment on the motor tests persisted to 15 months after CCI. See results in **Appendix A, Figure 3.**

- MRI/MRS 1 month after CCI, and 15 months after CCI

We found that mice who received a CCI had a substantial cortical cyst 1 month post injury, and showed evidence of chronic neurodegeneration with area of damage doubling in size from 1 to 15 months post CCI. See results in **Appendix A, Figure 3.**

- Age the mice

- Sacrifice mice and collect brain hemispheres 1 month and 15 months after CCI

- Perform mitochondrial enzyme assays

We found that complex I activity decreased with age in the injured cortex of CCI mice, but did not decrease with age in the contralateral hgemisphere. We did not see aging- or injury-related changes in other mitochondrial enzymes at 1 or 15 months post CCI. See results in **Appendix A, Figure 4.**

- Milestone Achieved: Manuscript prepared and submitted.

Specific Aim 3: we have completed all of the following tasks described in the SOW.

- Local IACUC Review/Approval

- ACURO Review/Approval

- Acquire mice: acquisition will be staggered (Total of 23 rTg4510 mice)

- Administer CCI

- Age the mice

- Collect hippocampus DNA 15 months following CCI

- Prepare frontal cortices for tangle analysis

- Analyze mitochondrial DNA copy number in mouse hippocampi*

We found that hippocampal mtDNAcn was lower on ipsilateral than the contralateral side 15 months after CCI in rTg4510 mice. See results in **Appendix A, Figure 7.**

**Note:* as described above, measuring mtDNAcn is an alternative approach we used to assess aging-related changes in brain mitochondria. We elected to move forward with this approach after extensive efforts to adapt existing methods for sequencing low-frequency mtDNA heteroplasmy failed to generate reliable results in the shrunken hippocampal samples collected from the injured/aged and transgenic mice in this study.

- Perform tangle analysis

We found that the number of tangle-bearing cells in the frontal cortex 15 months after CCI in rTg4510 mice was consistently lower on the side ipsilateral to injury. We did not detect significant correlations between mtDNAcn and tangle counts. See results in **Appendix A, Figure 7** and **Supplementary Figure 2**.

- Milestone Achieved: Manuscript prepared and submitted.

Opportunities for training and professional development provided by the project:

This project provided hands-on training and career development opportunities for three postdoctoral fellows in the Swerdlow laboratory and three graduate students in the Harris laboratory.

How were results were disseminated to communities of interest?

- Results have been prepared in a manuscript submitted and currently under review at the Journal of Neurotrauma (Appendix A)

- Preliminary results were shared by Dr. Harris with the scientific community in research talks given at:

- Uniformed Services University of the Health Sciences, Department of Anatomy, Physiology, and Genetics, Bethesda, MD (April 2021)
- Virginia Commonwealth University, Department of Anatomy and Neurobiology (Feb 2020)
- University of Kentucky webinar series, “Current Topics in TBI” (July 2020)

What do you plan to do during the next reporting period to accomplish the goals?

Nothing to Report.

4. Impact

What was the impact on the development of the principal discipline(s) of the project?

Our results indicate that mtDNA copy number increased with aging, and this effect was exaggerated in mice that had received a TBI. Thus, a TBI in early life appears to have accelerated an aging-associated process in the brain mitochondria. Further discussion of this cenral finding may be found in our manuscript (see Appendix A).

What was the impact on other disciplines?

Nothing to Report.

What was impact on technology transfer?

Nothing to Report.

What was the impact on society beyond science and technology?

Our project provides new insight into the connections between TBI, aging, and Alzheimer’s disease. For survivors of TBI and their families and caregivers, understanding these connections so that we can develop new therapeutic interventions is of the utmost importance.

5. Changes/Problems

Nothing to Report.

6. Products

A manuscript reporting the major study results has been submitted to the Journal of Neurotrauma and is under review.

A second manuscript reporting the novel protocols our team developed for deep sequencing of mitochondrial DNA microheteroplasmy is also in preparation.

7. Participants and other collaborating organizations

Year 1 Participants

Name:	Janna Harris
Project Role:	Multiple PI (Contact)

Research Identifier:	0000-0002-4829-6360
Nearest person month worked:	4.7 Calendar Months
Contribution to Project:	Dr. Harris obtained the Animal Protocol approvals from IACUC and ACURO. She has supervised work by study team members to optimize experimental protocols, and to source materials that will be needed, and to schedule and carry out animal experiments. She has coordinated meetings with the co-PI Dr. Swerdlow, as well as meetings with other individuals on the project.
Funding Support:	No change

Name:	Russell Swerdlow
Project Role:	Multiple PI
Research Identifier:	0000-0003-2948-7230
Nearest person month worked:	1.35 Calendar Months
Contribution to Project:	Dr. Swerdlow has worked collaboratively with co-PI Dr. Harris and the study team to supervise development of the study protocols and schedules, to troubleshoot when any issues arise, and to review the progress of animal experiments.
Funding Support:	No change

Name:	Xiaowan Wang
Project Role:	Postdoctoral Fellow
Research Identifier:	Not applicable
Nearest person month worked:	2.8 Calendar Months
Contribution to Project:	Dr. Wang has carried out the mouse behavioral studies, and worked to develop protocols for the mitochondrial enzyme assays, brain tissue dissection and isolation of total DNA, and tau tangle stereology.
Funding Support:	No change

Name:	Judit Perez-Ortiz
Project Role:	Postdoctoral Fellow
Research Identifier:	0000-0002-8953-4281
Nearest person month worked:	2.8 Calendar Months
Contribution to Project:	Dr. Perez-Ortiz has carried out the mouse behavioral studies, and worked to develop protocols for behavioral testing, brain tissue dissections, DNA isolation, and stereology analysis.
Funding Support:	No change

Name:	(Harry) Scott Barbay
Project Role:	Senior Scientist
Research Identifier:	0000-0003-2470-7775
Nearest person month worked:	3.0 Calendar Months
Contribution to Project:	Dr. Barbay assisted with preparation of the animal protocols and sourcing of research supplies. During the reporting period he completed 32 TBI/sham surgeries and assisted with animal health monitoring and medical records.
Funding Support:	No change

Name:	Sarah Christian
Project Role:	Research Assistant
Research Identifier:	Not applicable
Nearest person month worked:	10.2 Calendar Months
Contribution to Project:	Ms. Christian assisted with preparation of the animal protocols and development of experimental protocols for animal behavior

	assessments. She has also been responsible for sourcing and ordering research supplies, animal health monitoring, maintenance of study records and laboratory compliance.
Funding Support:	No change

Name:	DongWei Hui
Project Role:	Senior Research Associate
Research Identifier:	0000-0003-1020-8940
Nearest person month worked:	2.45 CYM
Contribution to Project:	Dr. Hui developed and optimized methodologies for mitochondrial DNA isolation from mouse brain and preparation for deep sequencing without contamination from nuclear DNA.
Funding Support:	No change

Year 2 Participants

Name:	Janna Harris
Project Role:	Multiple PI (Contact)
Research Identifier:	0000-0002-4829-6360
Nearest person month worked:	3.7 Calendar Months
Contribution to Project:	Dr. Harris has coordinated work by the study team to carry out all live animal experiments. She has supervised scheduling to keep the timeline on track, overseen data analysis, and coordinated meetings with co-PI Dr. Swerdlow and with other individuals on the project.
Funding Support:	No change

Name:	Russell Swerdlow
Project Role:	Multiple PI
Research Identifier:	0000-0003-2948-7230
Nearest person month worked:	1.2 Calendar Months
Contribution to Project:	Dr. Swerdlow has worked collaboratively with co-PI Dr. Harris and the study team to supervise execution of the study protocols, to review the progress of animal experiments, and to troubleshoot when issues arise.
Funding Support:	No change

Name:	Xiaowan Wang
Project Role:	Postdoctoral Fellow
Research Identifier:	Not applicable
Nearest person month worked:	4.4 Calendar Months
Contribution to Project:	Dr. Wang has carried out the mouse behavioral testing, euthanasia and brain tissue dissections, and has worked to refine protocols for the mitochondrial enzyme assays.
Funding Support:	No change

Name:	Judit Perez-Ortiz
Project Role:	Postdoctoral Fellow
Research Identifier:	0000-0002-8953-4281
Nearest person month worked:	4.7 Calendar Months
Contribution to Project:	Dr. Perez-Ortiz has carried out the mouse behavioral testing and data analysis, euthanasia and brain tissue dissections, and assisted with stereology protocols.

Funding Support:	No change

Name:	(Harry) Scott Barbay
Project Role:	Senior Scientist
Research Identifier:	0000-0003-2470-7775
Nearest person month worked:	3.0 Calendar Months
Contribution to Project:	Dr. Barbay assisted with preparation of the animal protocols and sourcing of research supplies. During the reporting period he completed 73 TBI/sham surgeries and assisted with ongoing animal health monitoring and medical records.
Funding Support:	No change

Name:	Sarah Christian
Project Role:	Research Assistant
Research Identifier:	Not applicable
Nearest person month worked:	9.0 Calendar Months
Contribution to Project:	Ms. Christian assisted with all TBI/sham surgical procedures, MRI scans, and animal behavior assessments. She has also been responsible for sourcing and ordering research supplies, monitoring the health of the mice, and maintaining study records and laboratory compliance.
Funding Support:	No change

Name:	DongWei Hui
Project Role:	Senior Research Associate
Research Identifier:	0000-0003-1020-8940
Nearest person month worked:	2.3 CYM
Contribution to Project:	Dr. Hui refined methodologies for mitochondrial DNA isolation from mouse brain and for deep sequencing without contamination from nuclear DNA.
Funding Support:	No change

Year 3 Participants

Name:	Janna Harris
Project Role:	Multiple PI (Contact)
Research Identifier:	0000-0002-4829-6360
Nearest person month worked:	3.5 Calendar Months
Contribution to Project:	Dr. Harris has coordinated work by the study team to carry out all proposed experiments. She has supervised scheduling and progress to keep the timeline on track, maintained regular communications with co-PI Dr. Swerdlow and other team members, and has worked on data analysis and interpretation.
Funding Support:	No change

Name:	Russell Swerdlow
Project Role:	Multiple PI
Research Identifier:	0000-0003-2948-7230
Nearest person month worked:	1.0 Calendar Months
Contribution to Project:	Dr. Swerdlow has worked collaboratively with co-PI Dr. Harris and the study team to supervise execution of the study protocols, to review the progress of animal experiments, to interpret findings, and to troubleshoot when issues arise.

Funding Support:	No change

Name:	Xiaowan Wang
Project Role:	Postdoctoral Fellow
Research Identifier:	n/a
Nearest person month worked:	5.0 Calendar Months
Contribution to Project:	Dr. Wang has carried out the mouse behavioral testing, euthanasia and brain tissue preparations, and has worked to refine protocols for the mitochondrial enzyme assays.
Funding Support:	No change

Name:	Anuradha Kalani
Project Role:	Postdoctoral Fellow
Research Identifier:	n/a
Nearest person month worked:	4.0 Calendar Months
Contribution to Project:	Dr. Kalani has assumed responsibility for carrying out the mitochondrial enzyme experiments and tau tangle stereology.
Funding Support:	No change

Name:	(Harry) Scott Barbay
Project Role:	Senior Scientist
Research Identifier:	0000-0003-2470-7775
Nearest person month worked:	3.0 Calendar Months
Contribution to Project:	Dr. Barbay assisted with preparation of the animal protocols and sourcing of research supplies. During the reporting period he assisted with animal health monitoring and medical records.
Funding Support:	No change

Name:	Sarah Christian
Project Role:	Research Assistant
Research Identifier:	n/a
Nearest person month worked:	12.0 Calendar Months
Contribution to Project:	Ms. Christian assisted with all TBI/sham surgical procedures, MRI scans, and animal behavior assessments. During the reporting period she was responsible for sourcing and ordering research supplies, monitoring the health of the mice, maintaining study records and compliance, and data analysis.
Funding Support:	No change

Name:	DongWei Hui
Project Role:	Senior Research Associate
Research Identifier:	0000-0003-1020-8940
Nearest person month worked:	1.0 Calendar Months
Contribution to Project:	Dr. Hui refined methodologies for mitochondrial DNA isolation from mouse brain without contamination from nuclear DNA, in preparation for deep sequencing to identify microheteroplasmies.
Funding Support:	No change

Year 4 (NCE) Participants

Name:	Janna Harris
Project Role:	Multiple PI
Research Identifier:	0000-0002-4829-6360
Nearest person month worked:	3.5 Calendar Months

Contribution to Project:	No Change

Name:	Russell Swerdlow
Project Role:	Multiple PI
Research Identifier:	0000-0003-2948-7230
Nearest person month worked:	1.0 Calendar Months
Contribution to Project:	No Change

Name:	Lesya Novikova
Project Role:	Senior Scientist
Research Identifier:	
Nearest person month worked:	3.5 Calendar Months
Contribution to Project:	Dr. Novikova carried out the tissue preservation, staining, and quantitative histopathology studies.

Name:	Dongwei Hui
Project Role:	Senior Scientist
Research Identifier:	0000-0003-1020-8940
Nearest person month worked:	1.0 Calendar Months
Contribution to Project:	No Change

8. SPECIAL REPORTING REQUIREMENTS

COLLABORATIVE AWARDS: For collaborative awards, independent reports are required from BOTH the Initiating PI and the Collaborating/Partnering PI. A duplicative report is acceptable; however, tasks shall be clearly marked with the responsible PI and research site. A report shall be submitted to https://ebrap.org External link for each unique award.

QUAD CHARTS: If applicable, the Quad Chart (available on https://www.usamraa.army.mil) should be updated and submitted with attachments.

9. APPENDICES:

Appendix A. “Traumatic Brain Injury Alters the Trajectory of Age-related Mitochondrial Change” submitted to the Journal of Neurotrauma, September 2023.

APPENDIX A

Traumatic Brain Injury Alters the Trajectory of Age-Related Mitochondrial Change

Janna L. Harris,[1,2] Xiaowan Wang,[1] Sarah K. Christian,[1] Lesya Novikova,[1] Anuradha Kalani,[1] Dongwei Hui,[1] Sadie Ferren,[1] Scott Barbay,[3] Judit Perez Ortiz,[1] Randolph J. Nudo,[3] William M. Brooks,[1,4] Heather M. Wilkins,[1,4] Prabhakar Chalise,[1,5] Mary Lou Michaelis,[1] Elias K. Michaelis,[1] Russell H. Swerdlow,[1,2,4,6,*]

1 University of Kansas Alzheimer's Disease Research Center, University of Kansas Medical Center, Kansas City, KS 66160
2 Department of Cell Biology & Physiology, University of Kansas Medical Center, Kansas City, KS 66160
3 Department of Physical Medicine & Rehabilitation, University of Kansas Medical Center, Kansas City, KS 66160
4 Department of Neurology, University of Kansas Medical Center, Kansas City, KS 66160
5 Department of Biostatistics & Data Science, University of Kansas Medical Center, Kansas City, KS 66160
6 Department of Biochemistry & Molecular Biology, University of Kansas Medical Center, Kansas City, KS 66160

*Corresponding Author: Russell H. Swerdlow, MD
KU Alzheimer's Disease Research Center
4350 Shawnee Mission Parkway
Fairway, Kansas 66205
rswerdlow@kumc.edu

Running Title: TBI and Brain Aging

Keywords: aging; Alzheimer's disease; brain; mitochondria; traumatic brain injury

Contact Information for Each Author:

Janna Harris	jharris2@kumc.edu
Xiaowan Wang	xwang9@kumc.edu
Sarah Christian	skcmv8@umkc.edu
Lesya Novikova	lnovikova@kumc.edu
Anuradha Kalani	anukalani@csjmu.ac.in
Dongwei Hui	feihe@ku.edu
Sadie Ferren	sadieland17@gmail.com
Scott Barbay	SBARBAY@kumc.edu
Judit Perez Ortiz	agatta22@gmail.com
Randy Nudo	RNUDO@kumc.edu
William Brooks	wbrooks@kumc.edu
Heather Wilkins	hwilkins@kumc.edu
Prabhakar Chalise	pchalise@kumc.edu
Mary Lou Michaelis	mlm@ku.edu
Eli Michaelis	emichaelis@ku.edu

Russell Swerdlow rswerdlow@kumc.edu

Abstract

Epidemiologic studies associate traumatic brain injury (TBI) with increased Alzheimer's disease risk, but the underlying mechanisms are unknown. As Alzheimer's disease is age-related and a TBI can precede its onset by decades, we hypothesized that TBI accelerates brain aging by altering age-related mitochondrial changes. To test this, we administered unilateral controlled cortical impact (CCI) or sham injuries to 5-month-old C57BL/6J and tau transgenic rTg4510 mice. In the non-transgenic mice we assessed behavior (1-5 days, 1 month, and 15 months), brain lesion (1 and 15 months), and mitochondria (1 and 15 months) after CCI/sham. CCI caused acute behavioral deficits that were substantially improved or fully resolved by 1-month post-injury. Protein-normalized complex I and cytochrome oxidase activities were not significantly altered by injury at 1 or 15 months post, although complex I activity in the CCI ipsilesional cortex showed an aging-related decline from 1 month to 15 months. Hippocampal mitochondrial DNA copy number (mtDNAcn) was not significantly altered by injury at 1 month, increased with age, and rose to the greatest extent in the CCI contralesional hippocampus. In the injured then aged rTg4510 mice, the ipsilesional hippocampus contained less mtDNA and fewer tangles relative to the contralesional hippocampus; mtDNAcn and tangle counts did not correlate. Overall, as mice age their brains increase mtDNAcn as part of a compensatory response to help preserve mitochondrial function. We found an enhanced aging-related mtDNAcn increase in brain-injured mice, suggesting that the amount of compensation required to preserve mitochondrial function late in life may be greater after a brain injury. TBI may, therefore, increase Alzheimer's disease risk by affecting the trajectory or biology of aging-related mitochondrial adaptation.

Introduction

Clinical, epidemiologic, and neuropathologic studies associate traumatic brain injury (TBI) with cognitive impairment.[1] Signs and symptoms can obviously present coincident with a TBI event but may also arise or evolve beyond their acute or even sub-acute occurrence. For example, repetitive brain injuries can cause a chronic and progressive neurologic disorder, chronic traumatic encephalopathy (CTE), that primarily manifests well after the period of injury acquisition.[2] Retrospective clinical studies also find a single, severe TBI increases one's lifetime risk of developing Alzheimer's disease,[3] the most common age-related neurologic disease and cause of late-life dementia. As is the case with CTE, the presumably responsible TBI can occur long before Alzheimer's disease clinical onset.[4]

The mechanisms that underlie the association between TBI in young or middle adulthood and increased late-onset Alzheimer's disease risk are unclear. It is possible a TBI event acutely or sub-acutely increases the production or aggregation, or both, of proteins that define Alzheimer's disease at the histology level. Consistent with this view are Alzheimer's disease transgenic mouse studies that find brain trauma alters the status of beta-amyloid (Aβ) and tau protein in those models.[5-7] Additional context is provided by biomarker studies of human subjects that show Aβ and tau levels and the histologic hallmarks they contribute to, amyloid plaques and neurofibrillary tangles, can change decades before cognitive decline develops.[8] If Aβ/plaques or tau/tangles slowly destroy the brain, then a TBI may directly initiate Alzheimer's disease through alterations in Aβ/plaques or tau/tangles, which then progressively damage the brain to the point that symptoms emerge decades later. Under this scenario, Alzheimer's disease is acquired at or near the time of the TBI, and simply takes time to clinically manifest.

An alternative view is that TBI does not directly confer Alzheimer's disease through changes in Aβ or tau protein, or through an induction of amyloid plaques and tau tangles, but rather indirectly increases Alzheimer's disease risk by accelerating or enhancing other Alzheimer's disease-permissive biologic phenomena such as brain aging. Alzheimer's disease incidence and prevalence markedly increase with age, and

the strong association between advancing age and Alzheimer's disease suggest the presence of a common underlying mechanism.[9]

Mitochondria are cell organelles that play a central role in bioenergetics and other essential cell functions. Mitochondrial alterations are recognized hallmarks of both aging and Alzheimer's disease,[10,11] and for this reason some propose mitochondria could mechanistically link or bridge these conditions.[12] Mitochondrial function is altered during the acute and post-acute stages of a TBI.[13-15] For these reasons, we considered the possibility that TBI may influence the trajectory or biology of age-related mitochondrial changes, and through this help explain the reported association between TBI and increased Alzheimer's disease risk.

Methods

Mice and procedural overview

The University of Kansas Medical Center Institutional Animal Care and Use Committee (Animal Care and Use Protocol #2018-2475), and the USAMRMC Animal Care and Use Review Office (ACURO) (protocol AZ170111.e001) approved all experimental animal protocols and procedures. The number of mice used for these studies was based on power calculations and mortality estimates, in which we anticipated a 30% attrition rate for head-injured mice maintained over the entire duration of the study.

We purchased 76 male, 4-month-old C57BL/6J mice and 23 male, 4-month-old rTg4510 mice from the Jackson Laboratory. The mice were acclimated to our vivarium for 3 weeks, group-housed to a maximum of 5 littermates per cage in Touch Slim Line IVC cages (Techniplast), and maintained on a 12-hour light/dark cycle. Some mice were separated on an individual basis upon recommendation of the institutional veterinary staff for excessive fighting; singly housed mice were provided additional nestlets for environmental enrichment.

The non-transgenic (non-tg) mice throughout received a standard chow diet (LabDiet product # 5053) with *ad libitum* access to food and water. The rTg4510 mice, which express a repressible form of human tau that contains a P301L mutation that drives intraneuronal tau fibril accumulation,[16] were maintained until 12 months of age on a doxycycline-enriched (200 mg/kg doxycycline hyclate) chow diet to repress transgene

expression. After that point, tau transgene expression was activated by switching these mice to the standard chow diet. The rTg4510 mice also had *ad libitum* access to food and water.

At 5 months of age the young adult, non-tg mice were randomized to receive either a controlled cortical impact (CCI) or sham surgery. All the 5-month-old rTg4510 mice received a CCI surgery. The non-tg mice were euthanized at either 6 (n=29; 14 shams) or 20 (n=44; 21 shams) months of age. We initially intended to age the tg mice to 20 months, but that cohort experienced higher than expected age-dependent mortality and the remaining mice (n=15) were euthanized at age 17.5 months.

Euthanasia was performed by isoflurane overdose, at which point the brains from the non-tg mice were rapidly removed and dissected. The parietal cortex and hippocampal regions were separated, designated as either ipsilesional or contralesional to CCI/sham and were placed in phosphate buffered saline (PBS) and immediately frozen at -80°C. The frontal lobes from the transgenic mice were formalin-fixed, embedded in paraffin, sectioned, mounted on slides, and stored at room temperature.

The parietal cortical regions were used for electron transport chain (ETC) assays, the hippocampi for mitochondrial DNA copy number (mtDNAcn) determinations, and the formalin-fixed frontal tissue for histologic analyses (described below). Performing biochemical and molecular assays on frozen rather than fresh tissue allowed us to analyze all the samples together and thus avoid batch-effect variation. The mice were also characterized through behavioral testing and brain magnetic resonance imaging (MRI), per protocols and schedules as described. All assessments of living non-tg mice, or on their collected tissues, were performed in a blinded fashion. Figure 1 summarizes the study design and timeline.

CCI and sham surgeries

A CCI targeting the right sensorimotor cortex was produced using a commercial impactor (Impact One Stereotaxic CCI Instrument, Leica Microsystems) as described in our previous publications.[17,18] Briefly, the device was mounted on a stereotaxic frame to reproduce the position and direction of the impact with high precision. Following anesthesia with isoflurane (3% induction, 1-2% maintenance) mice were immobilized in the stereotaxic frame and placed on a feedback-controlled heating pad to maintain core body temperature.

All surgeries were carried out by a single surgeon under aseptic conditions. The scalp was retracted, and a 4 mm diameter circular craniectomy was performed with a trephine bit (Patterson Dental), centered 0.5 mm anterior and -2.0 mm lateral to bregma. The impactor tip, which consisted of a 3 mm diameter stainless steel rod, was centered within the craniectomy, and angled so that the face of the impactor tip was tangential to the dural surface. The impactor tip was slowly lowered until contact with the dura was indicated by a contact sensor alarm. The tip was then retracted, and the trigger switch activated to deliver the cortical impact at 3.5 m/s, 2.0 mm depth, and 100 ms contact time. The cranial defect was repaired with a sterilized plastic cap secured with Vetbond adhesive. The incision was closed with 4-0 Vicryl sutures and treated with a topical analgesic (EMLA cream) and antibiotic ointment. Mice were removed from the stereotaxic frame and placed in a heated recovery chamber. The sham-injured control mice received an identical craniotomy, but the bone flap was left in place to avoid meningeal damage. The anesthesia duration for the sham surgeries was matched to that of the CCI surgeries.

Magnetic resonance imaging

MRI scans were obtained at 9.4T on 1-2% isoflurane-anesthetized mice maintained at a respiration rate of 100-150/minute; we used a feedback-controlled heating pad to keep core body temperature at 37 ºC. Gradient echo multi-slice images (TR = 65 ms, TE = 2.8 ms) were used to position the mouse's head in the magnet isocenter, followed by rapid acquisition with relaxation enhancement T_2-weighted images (TR = 4000 ms, TE = 0.01 ms, echo train length = 16, slices = 17, slice thickness = 0.5 mm). T_2-weighted images were analyzed with a semi-automated MatLab program developed in-house to quantify the TBI lesion using a modified Cavalieri approach.

Brain tissue loss was calculated by subtracting the contralesional hemisphere cerebrospinal fluid (CSF) volume from the ipsilesional hemisphere CSF volume in mm^3. To account for variance in brain volume between mice and within individual mice over the course of aging, we normalized the lesion to total brain volume in mm^3 obtained from the MR images. We compared sham, CCI, and tg-CCI mice at 1 month post injury and compared the change in brain lesion from 1 month to 15 months post-injury.

Behavioral assessments

We only performed behavioral assessments on the non-tg mice. The test battery included two motor tasks (rotarod, grid walk) and one cognitive task (Barnes maze). All behavioral assessments were conducted in the morning (8:00 – 11:00 am) and in the same order (Barnes, grid walk, rotarod) across testing days. At the start of the study, mice were acclimated to the behavioral apparatus for one day, then trained on the tasks for three days (days -5 to -3) to establish a reliable pre-injury performance baseline. After administering CCI or sham surgery, behavior was tested at an "acute" stage (days +1 to +4), a "recovery" stage (1 month post), and a "post-aging" stage (15 months post).

To perform the rotarod test, a four-lane rotarod apparatus (Accuscan, Mentor, OH) was set to accelerate from 4 to 40 rpm. On each day we ran three trials with at least 5 minutes of rest between trials. The average score of the trials from each day was used for analysis.

The grid walk test was conducted on a 20 cm wide by 35 cm long, 1.1 cm wire grid platform. Mice were placed on the grid and allowed to explore for 3 minutes while behavior was video recorded. Videos were analyzed to quantify time spent walking vs. motionless and the total number of foot faults in which the foot passed completely below the plane of the grid. For each session, a grid walk score was calculated from the number of contralesional foot faults divided by the total walking time. We normalized foot faults to actual walking time to account for differences in locomotion between sessions.

Barnes maze testing was conducted on a brightly illuminated white circular platform (90 cm diameter) with 20 holes (5 cm diameter) around the periphery. A dark escape box was placed under one of the holes. For each trial, the mouse was placed in an opaque start box in the center of the maze for 10 seconds before lifting the box to start the test. Our Barnes maze protocol consisted of 4 learning days followed by a probe day. On learning days, the mouse was placed in the center of the maze and allowed to explore for 2 minutes. On the probe day, the escape hatch was covered so the animal could not enter, and the mouse was allowed to explore for 1 minute. Performance was recorded using a ceiling mounted VideoTrack system (ViewPoint Systems).

Videos were analyzed for distance traveled and latency to reach the escape hatch on learning days, and for latency to reach the perimeter of the escape hatch on the probe trial day.

Electron transport chain Vmax assays

We used methods previously established by our group[19,20] to quantify mitochondrial complex I and complex IV (cytochrome oxidase; COX) Vmax enzyme activities. The assays were performed on homogenates of parietal cortex tissue from the non-tg mice. We specifically evaluated both parietal cortices from the CCI-injured mice, and the ipsilesional parietal cortex from the sham-injured mice at 1 and 15 months post CCI/sham. The amount of total protein present in each homogenate was determined using a BCA protein assay kit (BioRad, Hercules, CA), and the spectrophotometrically determined Vmax rate for each sample was normalized to its corresponding protein value. Readings were obtained using an Infinite M200 plate reader (Tecan). We performed an additional calculation in which we normalized each sample's Vmax/protein activity to the hippocampal mtDNAcn mean value for its corresponding sample group, or to the mtDNAcn from its corresponding hippocampal tissue (see below).

Mitochondrial DNA copy number determination

We performed mtDNAcn measurements on whole hippocampi. From the non-tg and rTg4510 mice that received a CCI we obtained both ipsilesional and contralesional data. From the non-tg sham mice we obtained only ipsilesional data. Our mtDNAcn sample sizes are slightly smaller than our ETC sample sizes as 2-3 hippocampal samples from each group were directed towards other applications, and one sample (in the sham 15-month group) could not be confidently identified.

Total genomic DNA was purified from 10 mg or less of brain tissue samples using a New England Biolabs Monarch Genomic DNA Purification Kit. The purified DNA was eluted in 100 µl of elution buffer, and the concentration in each sample measured using a Nanodrop 1000. The DNA was diluted to a concentration of 1 µg/mL in 1 mM Tris-HCl buffer, pH 8.5, containing 5 mM NaCl and 20 µg/µL *E. coli* DNA.

We estimated mtDNA to 18S rRNA DNA ratios following reverse transcription PCR (RT-PCR) using Promega GoTaq G2 Hot Start Master Mixes Colorless, Syto-82 (Thermo Fisher Scientific) 5 mM, 4µl/mL, and USB ROX Passive Reference Dye (Affymetrix 75768) 4 µl/mL.[21] One primer set was directed to the *Mus musculus* mitochondrial genome to generate a 180 base pair amplicon: mMitoF2 TCATCCTTCTCTCCCTATGAGGAAT (10948-10972) and mMitoR2 GGCCATGTGCGATTATTAGTATTGT (11103-11127). The other primer set was directed to the *Mus musculus* C57BL/6J chromosome 6, GRCm39 to generate a 144 bp amplicon: m18sF2 GTCGTAGTTCCGACCATAAACGATG (3201513-3201537) and m18sR2 TCCGTCAATTCCTTTAAGTTTCAGC (3201632-3201656). The total volume of the RT-PCR assays was 25 µL, the primer concentration was 0.5 µM, and the template DNA amount in each assay was 2 ng. The RT-PCR was carried out on an ABI 7500 fast PCR machine using the following program: stage 1, 95 ºC, 10 minutes; stage 2, 95 ºC for 10 seconds, 57 ºC for 10 seconds, and 65 ºC for 40 seconds for 50 cycles; stage 3, 95ºC for 15 seconds, 60ºC for 1 minute, and 95ºC for 15 seconds.

For each brain sample quadruplicate reactions of the mtDNA and 18S DNA targets were run in the same 96-well plate. A total of 12 brain samples were analyzed in each plate. The RT-PCR results were auto-analyzed (ABI 7500 Fast System SDS software, v1.3) and exported as a CVS data file that was used to calculate the mtDNA copy number relative to the 18S rRNA DNA.

Histopathology

Frontal cortices from nine of the 15 rTg4510 mice were suitable for tau histologic analysis, and five had enough residual tissue to also permit NeuN and glial fibrillary acid protein (GFAP) staining. We isolated the frontal cortex with a vertical cut at Bregma $\pm$1.2 mm then fixed with 4% paraformaldehyde in PBS for 4 days at 4°C. After fixing, the brain was embedded in paraffin wax using a Leica Biosystems ASP6025S tissue processor. The paraffin blocks were cut into 7 µm thick sections and mounted directly on Superfrost/Plus microscope slides (Fisher, # 12-550-15). The slides were dried at 40°C overnight and stored in slide boxes at

room temperature until further processing. Methodological details related to tissue processing, staining, and stereological analysis can be found in Supplementary Methods.

Statistics

The outcomes were summarized with respect to mean and standard error of the mean (SEM) for each defined group and bar plots of the means with error bars. Differences in outcomes between two independent groups of mice were assessed using two sample t-tests, and differences in outcomes from the same set of mice were assessed using paired t-tests. Comparisons of outcomes among three groups were performed using one-way analysis of variance (ANOVA) followed by Tukey's post-hoc test. The differences in the behavioral outcomes (rotarod, grid walk, Barnes maze) between the groups that were measured over time were assessed using a mixed effects modeling framework for repeated measures data using SAS procedure GLIMMIX. Spearman's rank correlation analyses were carried out to examine relationships between outcomes. P-values <0.05 were considered statistically significant.

Results

CCI produced brain lesions that evolved during aging

Long-term survival of the non-tg mice after injury was better than we predicted, while survival of the transgenic mice was worse than predicted. One mouse in the 1-month sham-injured group died following surgery; all the 1-month CCI mice survived. During the aging period, two non-tg mice from the 15-month sham-injured group died and did not contribute mtDNAcn or ETC data. All the CCI-injured mice survived the aging period. Eight out of the 23 transgenic mice died during the aging period (34.8%), and most of these deaths (6 out of 8) occurred during the period following removal of doxycyline at 12 months of age. Supplementary Figure 1 shows the number of mice that contributed to each component of the study.

We administered CCI or sham injuries to the right sensorimotor cortex of 5-month-old C57BL/6J and tau transgenic rTg4510 mice. One month later, MRI assessments showed a cystic brain lesion below the site of impact with ipsilesional hemisphere volume loss in the CCI mice, and essentially no observable structural

damage in the sham mice (Figure 2A,B). Mean absolute lesion volumes at 1 month were 0.24 ± 0.09 mm^3 in the sham group, 5.34 ± 3.16 mm^3 in the CCI group, and 7.19 ± 3.51 mm^3 in the tg-CCI group. Lesion volume normalized to total brain volume was larger in non-tg CCI group than in sham ($p < 0.0001$), and larger in the tg CCI group than in non-tg mice ($p=0.005$) even though the tau transgene expression was suppressed by doxycycline during this period (Figure 2C).

Over the 14-month aging period the normalized lesion volume increased by 73% in the sham-injured group. This change was statistically significant ($p =0.021$) although the area of damage remained very small in sham mice. Over the 14-month aging period the normalized lesion volume increased by 104% ($p<0.001$) in the non-tg CCI group (Figure 2D).

When the rTg4510 mice were 12 months old we removed the doxycycline from their chow to enable tau transgene expression. Around this time the transgenics began to lose weight and became increasingly frail (Figure 2E). For this reason, we did not obtain post-aging follow-up MRIs in the transgenic cohort.

CCI consistently and aging variably affected behavioral testing

The CCI affected rotarod test performance. In non-tg mice, rotarod performance 1-4 days post-CCI was markedly impaired relative to baseline and to the sham mice. At the 1-month time-point the CCI group rotarod performance improved, although not to the pre-injury level or to the level of the sham group. At the 15-month time-point the CCI group's rotarod performance was still slightly impaired. The relative difference between CCI and sham group performance at the 15-month timepoint was comparable to the relative amount of impairment at the 1-month timepoint. The sham group showed consistent rotarod performance across all measurements. (Figure 3A). In both groups, for unclear reasons rotarod performance on the first day of the post-aging evaluation differed from that of the subsequent testing days, but this aberration did not alter the outcome of the statistical analysis.

The CCI affected grid walk test performance. At all post-injury timepoints, the number of contralesional foot faults normalized to the total walking time was higher in CCI mice than in the sham-injured mice. The CCI-injured mice improved over time, performing better at 1 month than they did immediately after injury, and

better again at 15 months post. With aging there was a non-significant trend towards worsening performance in the sham group (p=0.168), but overall, the sham group performance remained consistent throughout the study (Figure 3C).

The CCI affected performance on the Barnes maze acutely after injury. During the immediate post-injury period the distance traveled and latency to goal scores were worse in the CCI group than they were in the sham group (p=0.033 and p=0.010). These deficits were no longer apparent at the 1-month post-injury time-point. At 15-months post-injury the distance traveled and latency to goal scores were not as good as they were at the 1-month time-point, but the extent of change with aging was comparable between the CCI and sham groups (Figure 3C,D). During the Barnes probe trial when the escape hatch was removed, CCI and sham mice had similar latency to goal scores acutely, 1 month, and 15 months post-injury (Figure 3E).

CCI accelerated the trajectory of age-related mitochondrial change

To determine whether TBI affected the trajectory of aging-related mitochondrial changes, we measured complex I and COX Vmax activities in the parietal cortex from CCI and sham non-tg mice. These assays were performed using brain homogenates in which we normalized enzyme-driven, time-dependent spectrophotometric changes to total protein. One month post-injury, complex I and COX activities were equivalent among the sham contralesional, CCI contralesional, and CCI ipsilesional tissues (Figure 4A,B); the CCI ipsilesional and CCI contralesional values remained comparable by paired t-test analysis. The complex I and COX activities were also equivalent among all three groups at the 15-month post-injury time-point (Figure 4C,D); the CCI ipsilesional and CCI contralesional values remained comparable by paired t-test analysis. Finally, we considered whether aging affected the enzyme activities. At 15 months post-injury, the complex I activity in the ipsilesional, injured hemispheres of the CCI mice was lower than it was at 1 month (21% reduction, p=0.036) (Figure 4E). We did not observe any other differences between the 1-month and 15-month enzyme activity means (Figure 4F-H).

To further assess the impact of TBI on the trajectory of age-related mitochondrial changes, we measured mtDNAcn in the hippocampi from CCI and sham non-tg mice. One month post-injury, mtDNAcn values were

equivalent among the sham ipsilesional, CCI ipsilesional, and CCI contralesional hippocampi (Figure 5A). Over the next 14 months the mtDNAcn increased in all groups, and in the old mice the mtDNAcn of the CCI contralesional samples exceeded that of the CCI ipsilesional and sham samples (Figure 5A). We further characterized the extent of each group's age-related increase as a percentage change over 14 months. In this analysis there was a non-significant trend towards a greater age-related increase in the CCI ipsilesional group vs sham (42% increase in sham brains vs. 57% increase in CCI-ipsilesional; $p=0.136$). The age-related increase in the CCI-contralesional group (78% increase) significantly exceeded that of the sham group ($p=0.002$) and that of the CCI-ipsilesional group ($p<0.001$) (Figure 5B).

Figure 5C emphasizes the age-dependent trajectory of the hippocampal mtDNAcn changes in the different groups. A TBI administered during young adulthood appeared to accelerate an age-related increase in hippocampal mtDNAcn, although this acceleration was not as robust on the injured side of the brain as it was on the contralesional side.

To add context to the question of how aging affected our TBI model we more closely examined the effects of aging itself in our sham control group. In the sham-injured mice, we jointly analyzed the ipsilesional hippocampus mtDNAcn and contralesional parietal cortex enzyme activity measurements presented in Figures 4 and 5. Between 6 and 20 months of age, the mtDNAcn in the brains of these mice increased by 42%. Their mtDNAcn, when normalized to nuclear DNA copy number, increased from a value of 31 to a value of 44 (Figure 6A), while complex I and COX activities, when normalized to total protein, did not change (Figure 6B,C). Further normalizing the complex I/protein and COX/protein enzyme activities to the mtDNAcn means, though, resulted in robust age-related differences (Figure 6B,C). Specifically, the complex I/protein/mtDNAcn value was 34% lower at 20 months of age than it was at 6 months, and the COX/protein/mtDNAcn value was 37% lower at 20 months of age than it was at 6 months. For each brain where we had both an ETC Vmax and mtDNAcn value ($n=12$ for the young mice; $n=17$ for the old mice) we also normalized the Vmax activity to the corresponding mtDNAcn value, and again the mtDNAcn-referenced activities were lower in the old mice (Figure 6D,E). This suggests that as the mice aged, to maintain brain complex I and COX activity homeostasis they needed to increase their brain mtDNAcn.

CCI-injured tau transgenic mice showed ipsi versus contralesional differences in mtDNA copy number and tangle counts

We intended to age the tau tg rTg4510 mice for 15 months after CCI and then assess mtDNAcn and tau tangle frequency, but the cohort exhibited progressive mortality causing us to end the study at 12.5 months post-injury (age 17.5 months). At this post-aging time point, mean mtDNAcn in the contralesional hippocampus was 16% higher than on the ipsilesional side (34.3 for contralesional vs. 29.6 for ipsilesional; p=0.015 by paired t-test) (Figure 7A). There was a positive correlation between the ipsilesional and contralesional mtDNAcn values from the individual mice (Supplementary Figure 2).

In the rTg4510 mice 12.5 months post-injury, we identified frontal cortex neurofibrillary tangles through thioflavin fluorescence and immunofluorescence (IF) with the S396 antibody that binds phosphorylated tau. For both hemispheres the number of tangle-bearing cells was greater with thioflavin than with the P396 antibody, and there were cells that were positive for one or both stains (Figure 7B,C). The number of thioflavin, P396, or co-stained cells was consistently greater in the frontal cortex contralesional to CCI (Figure 7C). We did not detect significant correlations between mtDNAcn and tangle counts (Supplementary Figure 2).

Five of the transgenic mouse frontal lobe blocks contained adequate residual tissue for neuronal and glial assessments, and in these we counted the number of DAPI-positive cells with clear concomitant NeuN or GFAP staining. We also measured the ipsilesional and contralesional NeuN and GFAP fluorescence intensities. We did not observe inter-hemispheral differences in neuron number, glial number, NeuN intensity, or GFAP intensity (Figure 7D).

Discussion

In this study we demonstrate that mouse hippocampus mtDNAcn increased between 6 and 20 months of age and administering a brain injury during young adulthood magnified this increase. Despite this age-related, TBI-enhanced mtDNAcn increase, brain complex I and COX activities remained relatively constant. The mitochondrial genome encodes proteins critical for oxidative phosphorylation, is present in numerous copies per

cell, and cellular levels of mtDNA are adjusted according to metabolic needs.[22] Accordingly, the most straightforward interpretation of our results is that the observed age-related, TBI-enhanced mtDNAcn increase is a compensatory change that helps brain mitochondria maintain a state of functional homeostasis, and that injured brains require more compensation during aging than non-injured brains.

Others report mouse brain mitochondria ETC activities decline with advancing age, but this is not a consistent finding.[13,23,24] Our protein-normalized complex I and COX activity data in sham-injured control mice do not reveal an age-related functional decline, which could reflect insufficient ETC assay sensitivity, the utilization of insufficiently aged mice, or resilience of the utilized strain to age-related functional declines. Our ETC data, though, remain consistent with the existing positive literature in that we do see evidence of an age-related decline in mitochondrial efficiency, as indicated by the observation that mitochondria in the brains of the old mice require more mtDNA to maintain a constant level of ETC function.

We performed our brain ETC and mtDNAcn measurements on bulk tissue, as opposed to a specific cell type. Relative to other brain cell types, neurons maintain a high mtDNAcn and their mitochondria are configured to perform respiration. Neuron loss, therefore, would predictably decrease, not increase, the bulk tissue mtDNAcn. Neuron loss could also potentially reduce the apparent activity of an ETC enzyme in bulk tissue.

Our data suggest the CCI affected mitochondria throughout the brain, including the contralesional hemisphere. If the age-related increase in brain mtDNAcn compensates for an age-associated decline in mitochondrial efficiency, one might expect the more damaged ipsilesional hemisphere would require more compensation and, accordingly, acquire a higher mtDNAcn than the contralesional side. We can only speculate as to why this was not the case, but potential explanations include the possibility that compensation potential is intrinsically reduced in the most severely injured areas, or that the injured hemisphere is subject to structural changes such as neuronal loss and gliosis that also affect mtDNAcn. Consistent with the latter scenario, we found the CCI injury increased the amount of age-associated volume loss in the ipsilesional hemisphere compared to sham, and the ipsilesional hemisphere complex I activity (normalized to protein) was lower 15 months post-injury than it was 1-month post-injury. Conversely, it is worth considering whether sensorimotor

dysfunction in the contralesional limbs increased reliance on the ipsilesional limbs, which then caused compensatory structural or mitochondrial changes in the contralesional hemisphere that manifested as an increased mtDNAcn. Studies in rats are variably consistent with this explanation.[25-27]

Other studies report mitochondrial function is altered during the acute stage of a TBI.[13,14] Investigators especially note mitochondria are major producers of oxidative stress, and oxidative stress markers rise immediately post-injury.[13,28] We did not determine whether the CCI injury in our study acutely affected brain mtDNAcn or ETC activities, but if it did those changes resolved within 1-month of the injury. If there were acute changes to these parameters, it would not change our conclusion that the CCI injury altered the trajectory of age-related mitochondrial change.

Our data do not address the mechanisms through which the CCI influenced aging-related mitochondrial change. It is possible the mtDNAcn increase is a response to some mtDNA-independent mitochondrial or even non-mitochondrial pathology. Alternatively, an injury-induced modification of the mtDNAcn itself may drive the effect. To this point the study of Barrientos et al., who reported human brain mtDNAcn increases with advancing age while mtDNA-derived transcripts decrease, is relevant.[29] The authors speculated the mtDNAcn increase they observed was an adaptive response to declining mtDNA expression efficiency. While the underlying basis for such a decline is unclear, it was recently reported that brains from Alzheimer's disease patients preferentially accumulate somatic mutations in the mtDNA control region that initiates mtDNA transcription.[30]

The brain cavitation and acute behavioral deficits we observed confirm moderate severity of the CCI injury. Despite the residual structural injury, within 1 month of the injury behavioral test performance recovered substantially. Over the aging period, although the CCI lesions continued to evolve, performance on the motor-based behavioral tests remained stable (rotarod) or improved (gridwalk), while the cognition-based behavioral test (Barnes maze) performance declined to the same extent as in the sham-injured mice. The difference in Barnes maze performances evident between the 6- and 20-month-old CCI mice, therefore, appears to represent an age rather than injury-related change. In general, though, preserved ETC function reflected preserved

behavioral function, raising the possibility that the mtDNAcn increase we believe directly supported mitochondrial function may have, by extension, also supported behavioral function.

Mitochondria are altered in Alzheimer's disease patients.[11] Relationships exist between the classic Alzheimer's disease histologies, the plaques and tangles, and mitochondria and cause-and-effect directionality is a matter of debate.[31] The non-tg mice we studied do not develop plaques or tangles, and therefore plaques or tangles cannot account for the observed age-related increase in their mtDNAcn. It is possible injury-induced changes in mouse amyloid precursor protein (APP), non-aggregated Aβ, or non-aggregated tau protein influenced mitochondrial efficiency and mtDNAcn changes, but our sham-injured mice showed similar mitochondrial dynamics. For this reason, unless APP, non-aggregated Aβ, or tau protein primarily drive brain aging in C57BL/6 mice, they probably cannot account for our observations in the CCI-injured non-tg mice.

Several studies report mitochondrial dysfunction promotes neurofibrillary tangle acquisition.[32-38] The rTg4510 mice we analyzed showed no evidence for this, as the directly injured hemisphere contained fewer tangles than the contralesional hemisphere and we did not detect relationships between mtDNAcn and tangle number. Our rTg4510 mouse data, though, are difficult to interpret as we do not know whether tangle formation was enhanced in the contralesional hemisphere, mitigated in the directly injured hemisphere, or artifactually altered by structural changes to the directly injured tissue. Our cell count data, however, suggest that a simple change in the number of ipsilesional neurons or astrocytes is not responsible. Also, in our experimental model the constitutive expression of a mutant human tau transgene over 5.5 months, in a previously head-injured mouse, could potentially introduce unrecognized artifacts.

The mtDNAcn of the 17.5-month-old tg mice was numerically closer to the mtDNAcn of the 6-month-old non-tg mice than it was to that of the 20-month-old non-tg mice. However, we did not measure the mtDNAcn in the young rTg4510 mice before transgene activation or immediately after transgene activation, mtDNAcn varies between mouse strains, and we don't know the impact of the transgene on mtDNAcn. We therefore cannot speculate on the trajectory of age-related mitochondrial or mtDNAcn changes in the rTg4510 mice and did not attempt to compare tg mouse mtDNAcn with non-tg mouse mtDNAcn.

Our data are relevant to human studies that report inherited mtDNA variation associates with TBI outcome. One study found specific mtDNA polymorphisms associate with the extent of recovery one year after TBI.[39] Another found TBI outcomes associate with mtDNA haplogroups defined by specific patterns of co-inherited mtDNA polymorphisms.[40] Per Bulstrode et al, haplogroup K carriers show better long-term TBI outcomes than those with other haplogroups,[40] which is consistent with studies that associate haplogroup K with reduced overall and especially APOE4-conferred Alzheimer's disease risk.[41-43] Our data are also relevant to the study of Gilmer et al, which found that immediately after a TBI brain mitochondrial dysfunction is more pronounced in old versus young rats.[13] The authors proposed this could at least partly explain why advancing age reduces the potential for TBI recovery. Collectively, these studies suggest baseline mitochondrial function and reserve capacity influence TBI short-and-long term outcomes. Our data further stress that mitochondrial compensation is part of brain aging, and TBI increases the amount of compensation that the aging process requires.

Data from experimental models may not always extrapolate beyond the model and can misinform the questions they were intended to address. To this point, we do not yet know the extent to which mitochondria and brain aging relationships differ between mice and humans. Although our data suggest a mechanistic link between TBI, mitochondria, and brain aging (at least in mice), the specific mechanisms that underlie or create this link were not addressed. While it is tempting to speculate that a TBI-induced burst of oxidative stress modified mtDNA bases to generate mtDNA mutations, our study did not test this. Our data identify a mechanism that could conceptually link TBI to Alzheimer's disease risk, but establishing the actual contribution and relevance of this mechanism is beyond the scope of our study. Finally, to support our major conclusions we referenced ETC activities to mtDNAcn, relying on the assumption that these measures are functionally interrelated. Future studies will be needed to experimentally address the complexities of the assumed ETC-mtDNAcn relationship.

Conclusions

Our study provides new insight into the relationships between TBI, mitochondria, brain aging, and Alzheimer's disease. To place these findings within a broader context, we speculate the aging brain uses compensatory mechanisms to maintain mitochondrial function, and a TBI increases the amount of compensation required to maintain mitochondrial function. When the amount of required compensation exceeds the ability to compensate, mitochondria homeostasis fails, and Alzheimer's disease may result. A TBI acquired during young adulthood may, therefore, increase the risk of late-onset Alzheimer's disease by promoting a mismatch between the amount of mitochondrial compensation the aging brain requires and its capacity for compensation.

Transparency, Rigor, and Reproducibility Statement

The USAMRMC Animal Care and Use Review Office (ACURO) (protocol AZ170111.e001) approved all experimental animal protocols and procedures; aside from IACUC institutional approval we did not register this study elsewhere. The number of mice used for these studies was based on power calculations and mortality estimates, in which we anticipated a 30% attrition rate for head-injured mice maintained over the entire duration of the study and which would provide >80% power to detect outcome differences were they to exist. The study was performed using 76 male, 4-month-old C57BL/6J mice and 23 male, 4-month-old rTg4510 mice purchased from the Jackson Laboratory. The number of mice allocated to each group and the number of mice providing data for each outcome is illustrated in detail in supplementary figure 1. Differences in outcomes between two independent groups of mice were assessed using two sample t-tests, and differences in outcomes from the same set of mice were assessed using paired t-tests. Comparisons of outcomes among three groups were performed using one-way analysis of variance (ANOVA) followed by Tukey's post-hoc test. The differences in the behavioral outcomes (rotarod, grid walk, Barnes maze) between the groups that were measured over time were assessed using a mixed effects modeling framework for repeated measures data using SAS procedure GLIMMIX. Spearman's rank correlation analyses were carried out to examine relationships between outcomes. P-values <0.05 were considered statistically significant. Data from the mtDNAcn analysis were generated from two assay batches, while all other data were generated simultaneously (ETC Vmax data, histology assessments) or continuously (behavioral and MRI data). Those performing outcome assessments were blinded to group.

Where antibodies were used, binding specificity was assessed through control assays that featured the absence of the primary antibody. No replication studies are planned by our group. Upon reasonable request, the data described in this study are available from the corresponding author.

Acknowledgments

The authors acknowledge the support of the University of Kansas Alzheimer's Disease Research Center, the Hoglund Biomedical Imaging Center, and the University of Kansas Medical Center Rodent Behavior Facility.

Authors' Contributions

JLH and RHS conceived the project and designed the experiments with input from RJN, WMB, HMW, MLM, and EKM. XW, SKC, LN, AK, DH, SF, JPO, and SB performed the procedural work and generated the data. JLH, PC, and RHS analyzed the data with contributions from EKM and DH (mtDNAcn), XW and SKC (mouse behavior), LN (immunofluorescence and thioflavin staining), and AK (ETC assays). JLH and RHS interpreted the data and wrote the manuscript with contributions from RJN, WMB, HMW, PC, MLM, and EKM. All authors read, edited, and approved the final manuscript.

Funding Information

This work was supported by DOD W81XWH-18-1-0497 and P30AG072973 (University of Kansas Alzheimer's Disease Research Center). RHS also receives support from the Thompson Foundation, the Dow Family Foundation, Clune Family Foundation, and the Snyder Family Foundation. The Hoglund Biomedical Imaging Center is supported by the Hoglund Family Foundation.

Author Disclosure Statement

The authors report no competing interests.

Supplementary Material

Supplementary material is available online.

References

1. Rabinowitz AR, Levin HS. Cognitive sequelae of traumatic brain injury. *Psychiatr Clin North Am*. Mar 2014;37(1):1-11. doi:10.1016/j.psc.2013.11.004
2. McKee AC. The Neuropathology of Chronic Traumatic Encephalopathy: The Status of the Literature. *Semin Neurol*. Aug 2020;40(4):359-369. doi:10.1055/s-0040-1713632
3. Julien J, Joubert S, Ferland MC*, et al*. Association of traumatic brain injury and Alzheimer disease onset: A systematic review. *Ann Phys Rehabil Med*. Sep 2017;60(5):347-356. doi:10.1016/j.rehab.2017.03.009
4. Haarbauer-Krupa J, Pugh MJ, Prager EM, Harmon N, Wolfe J, Yaffe K. Epidemiology of Chronic Effects of Traumatic Brain Injury. *J Neurotrauma*. Dec 2021;38(23):3235-3247. doi:10.1089/neu.2021.0062
5. Szczygielski J, Mautes A, Steudel WI, Falkai P, Bayer TA, Wirths O. Traumatic brain injury: cause or risk of Alzheimer's disease? A review of experimental studies. *J Neural Transm (Vienna)*. Nov 2005;112(11):1547-64. doi:10.1007/s00702-005-0326-0
6. Tran HT, LaFerla FM, Holtzman DM, Brody DL. Controlled cortical impact traumatic brain injury in 3xTg-AD mice causes acute intra-axonal amyloid-β accumulation and independently accelerates the development of tau abnormalities. *J Neurosci*. Jun 29 2011;31(26):9513-25. doi:10.1523/jneurosci.0858-11.2011
7. Edwards G, 3rd, Zhao J, Dash PK, Soto C, Moreno-Gonzalez I. Traumatic Brain Injury Induces Tau Aggregation and Spreading. *J Neurotrauma*. Jan 1 2020;37(1):80-92. doi:10.1089/neu.2018.6348
8. Jack CR, Jr., Knopman DS, Jagust WJ*, et al*. Hypothetical model of dynamic biomarkers of the Alzheimer's pathological cascade. *Lancet Neurol*. Jan 2010;9(1):119-28. doi:S1474-4422(09)70299-6 [pii]10.1016/S1474-4422(09)70299-6 [doi]

9. Swerdlow RH. Is aging part of Alzheimer's disease, or is Alzheimer's disease part of aging? *Neurobiol Aging*. Oct 2007;28(10):1465-80. doi:S0197-4580(06)00235-1 [pii]10.1016/j.neurobiolaging.2006.06.021 [doi]

10. Lopez-Otin C, Blasco MA, Partridge L, Serrano M, Kroemer G. The hallmarks of aging. *Cell*. Jun 6 2013;153(6):1194-217. doi:10.1016/j.cell.2013.05.039

11. Swerdlow RH. Mitochondria and cell bioenergetics: increasingly recognized components and a possible etiologic cause of Alzheimer's disease. *Antioxid Redox Signal*. Jun 15 2012;16(12):1434-55. doi:10.1089/ars.2011.4149

12. Swerdlow RH. The Alzheimer's Disease Mitochondrial Cascade Hypothesis: A Current Overview. *J Alzheimers Dis*. 2023;92(3):751-768. doi:10.3233/jad-221286

13. Gilmer LK, Ansari MA, Roberts KN, Scheff SW. Age-related mitochondrial changes after traumatic brain injury. *J Neurotrauma*. May 2010;27(5):939-50. doi:10.1089/neu.2009.1181

14. Gilmer LK, Roberts KN, Joy K, Sullivan PG, Scheff SW. Early mitochondrial dysfunction after cortical contusion injury. *J Neurotrauma*. Aug 2009;26(8):1271-80. doi:10.1089/neu.2008.0857

15. Lyons DN, Vekaria H, Macheda T*, et al*. A Mild Traumatic Brain Injury in Mice Produces Lasting Deficits in Brain Metabolism. *J Neurotrauma*. Oct 15 2018;35(20):2435-2447. doi:10.1089/neu.2018.5663

16. Spires TL, Orne JD, SantaCruz K*, et al*. Region-specific dissociation of neuronal loss and neurofibrillary pathology in a mouse model of tauopathy. *Am J Pathol*. May 2006;168(5):1598-607. doi:10.2353/ajpath.2006.050840

17. Onyszchuk G, Al-Hafez B, He YY, Bilgen M, Berman NE, Brooks WM. A mouse model of sensorimotor controlled cortical impact: characterization using longitudinal magnetic resonance imaging, behavioral assessments and histology. *J Neurosci Methods*. Mar 15 2007;160(2):187-96. doi:10.1016/j.jneumeth.2006.09.007

18. Guggenmos DJ, Azin M, Barbay S*, et al*. Restoration of function after brain damage using a neural prosthesis. *Proc Natl Acad Sci U S A*. Dec 24 2013;110(52):21177-82. doi:10.1073/pnas.1316885110

19. Ghosh S, Patel N, Rahn D*, et al*. The thiazolidinedione pioglitazone alters mitochondrial function in human neuron-like cells. *Mol Pharmacol*. Jun 2007;71(6):1695-702. doi:mol.106.033845 [pii]10.1124/mol.106.033845 [doi]

20. Parker WD, Jr., Parks JK, Swerdlow RH. Complex I deficiency in Parkinson's disease frontal cortex. *Brain Res*. Jan 16 2008;1189:215-8. doi:S0006-8993(07)02581-4 [pii]10.1016/j.brainres.2007.10.061 [doi]

21. Gudnason H, Dufva M, Bang DD, Wolff A. Comparison of multiple DNA dyes for real-time PCR: effects of dye concentration and sequence composition on DNA amplification and melting temperature. *Nucleic Acids Res*. 2007;35(19):e127. doi:10.1093/nar/gkm671

22. Filograna R, Mennuni M, Alsina D, Larsson NG. Mitochondrial DNA copy number in human disease: the more the better? *FEBS Lett*. Apr 2021;595(8):976-1002. doi:10.1002/1873-3468.14021

23. Boveris A, Navarro A. Brain mitochondrial dysfunction in aging. *IUBMB life*. May 2008;60(5):308-14. doi:10.1002/iub.46 [doi]

24. Navarro A, Boveris A. The mitochondrial energy transduction system and the aging process. *Am J Physiol Cell Physiol*. Feb 2007;292(2):C670-86.

25. Allred RP, Jones TA. Experience--a double edged sword for restorative neural plasticity after brain damage. *Future Neurol*. Mar 1 2008;3(2):189-198. doi:10.2217/14796708.3.2.189

26. Jones TA, Liput DJ, Maresh EL*, et al*. Use-dependent dendritic regrowth is limited after unilateral controlled cortical impact to the forelimb sensorimotor cortex. *J Neurotrauma*. May 1 2012;29(7):1455-68. doi:10.1089/neu.2011.2207

27. Nudo RJ. Postinfarct cortical plasticity and behavioral recovery. *Stroke*. Feb 2007;38(2 Suppl):840-5. doi:10.1161/01.STR.0000247943.12887.d2

28. Sullivan PG, Keller JN, Mattson MP, Scheff SW. Traumatic brain injury alters synaptic homeostasis: implications for impaired mitochondrial and transport function. *J Neurotrauma*. Oct 1998;15(10):789-98. doi:10.1089/neu.1998.15.789

29. Barrientos A, Casademont J, Cardellach F, Estivill X, Urbano-Marquez A, Nunes V. Reduced steady-state levels of mitochondrial RNA and increased mitochondrial DNA amount in human brain with aging. *Brain Res Mol Brain Res*. Dec 15 1997;52(2):284-9. doi:S0169328X97002787 [pii]

30. Harerimana NV, Paliwali D, Romero-Molina C*, et al*. The role of mitochondrial genome abundance in Alzheimer's disease. *Alzheimers Dement*. May 2023;19(5):2069-2083. doi:10.1002/alz.12812

31. Swerdlow RH. The Alzheimer's Disease Mitochondrial Cascade Hypothesis: A Current Overview. *J Alzheimers Dis*. Feb 11 2023;doi:10.3233/jad-221286

32. Blass JP, Baker AC, Ko L, Black RS. Induction of Alzheimer antigens by an uncoupler of oxidative phosphorylation. *Arch Neurol*. Aug 1990;47(8):864-9.

33. Escobar-Khondiker M, Hollerhage M, Muriel MP*, et al*. Annonacin, a natural mitochondrial complex I inhibitor, causes tau pathology in cultured neurons. *J Neurosci*. Jul 18 2007;27(29):7827-37. doi:27/29/7827 [pii]10.1523/JNEUROSCI.1644-07.2007 [doi]

34. Hoglinger GU, Lannuzel A, Khondiker ME*, et al*. The mitochondrial complex I inhibitor rotenone triggers a cerebral tauopathy. *J Neurochem*. Nov 2005;95(4):930-9. doi:JNC3493 [pii]10.1111/j.1471-4159.2005.03493.x [doi]

35. Hoglinger GU, Melhem NM, Dickson DW*, et al*. Identification of common variants influencing risk of the tauopathy progressive supranuclear palsy. *Nat Genet*. Jul 2011;43(7):699-705. doi:10.1038/ng.859

36. Hollerhage M, Deck R, De Andrade A*, et al*. Piericidin A aggravates Tau pathology in P301S transgenic mice. *PLoS One*. 2014;9(12):e113557. doi:10.1371/journal.pone.0113557

37. Rottscholl R, Haegele M, Jainsch B*, et al*. Chronic consumption of Annona muricata juice triggers and aggravates cerebral tau phosphorylation in wild-type and MAPT transgenic mice. *J Neurochem*. Aug 29 2016;doi:10.1111/jnc.13835

38. Yamada ES, Respondek G, Mussner S*, et al*. Annonacin, a natural lipophilic mitochondrial complex I inhibitor, increases phosphorylation of tau in the brain of FTDP-17 transgenic mice. *Exp Neurol*. Mar 2014;253:113-25. doi:10.1016/j.expneurol.2013.12.017

39. Conley YP, Okonkwo DO, Deslouches S*, et al*. Mitochondrial polymorphisms impact outcomes after severe traumatic brain injury. *J Neurotrauma*. Jan 1 2014;31(1):34-41. doi:10.1089/neu.2013.2855

40. Bulstrode H, Nicoll JA, Hudson G, Chinnery PF, Di Pietro V, Belli A. Mitochondrial DNA and traumatic brain injury. *Ann Neurol*. Feb 2014;75(2):186-95. doi:10.1002/ana.24116

41. Swerdlow RH, Hui D, Chalise P*, et al*. Exploratory analysis of mtDNA haplogroups in two Alzheimer's longitudinal cohorts. *Alzheimers Dement*. Aug 2020;16(8):1164-1172. doi:10.1002/alz.12119

42. Carrieri G, Bonafe M, De Luca M*, et al*. Mitochondrial DNA haplogroups and APOE4 allele are non-independent variables in sporadic Alzheimer's disease. *Hum Genet*. Mar 2001;108(3):194-8.

43. Maruszak A, Safranow K, Branicki W*, et al*. The impact of mitochondrial and nuclear DNA variants on late-onset Alzheimer's disease risk. *J Alzheimers Dis*. 2011;27(1):197-210. doi:10.3233/jad-2011-110710

Figure Legends

Figure 1. Overview of study flow and procedures. (A) Timeline for the non-tg mouse experiments. (B) Timeline for the tg mouse experiments.

Figure 2. Brain structure and volume changes. (A) A representative MRI taken 1 month after sham surgery shows the sham procedure did not grossly alter brain structure. (B) A representative MRI taken 1 month after CCI shows a cystic lesion underlying the region of impact. (C) Brain lesions were quantified 1-month post-injury as the volume of the contralesional hemisphere CSF subtracted from the volume of the ipsilesional hemisphere CSF and normalized to total brain volume. Normalized lesions were larger in the tg CCI group than in non-tg mice ($p < 0.05$) even though the tau transgene expression was suppressed by doxycycline during this period. (D) Over the course of the 14-month aging period the brain lesions continued to expand, increasing much more in non-tg CCI mice than in the sham-injured mice. (E) Increasing frailty of the tg mice, reflected here by premature weight loss, prompted us to forego post-aging MRI in the tg cohort.

Figure 3. Behavioral testing. (A) On the rotarod test, the CCI group showed impaired performance in the immediate post-injury period ($p<0.0001$). Their performance improved over the next month but did not return to the level of the sham group ($p=0.006$). Fifteen months post-injury the CCI mice rotarod performance did not show further change ($p=0.010$). The sham group showed consistent rotarod performance across all measurement periods. (B) On the grid walk test, relative to sham-injury, a CCI injury increased the number of left foot faults normalized to the total walking time. This deficit persisted through the acute ($p<0.0001$), 1-month ($p<0.0001$), and 15-months ($p<0.0001$) post injury timepoints. (C) In the Barnes maze, latency to goal for the CCI group was prolonged in the immediate post-injury period ($p=0.010$) but recovered over the next month to match the sham group time ($p=0.702$). The latency to goal time did increase over the subsequent 14-month aging period, although this change was comparable between the CCI and sham groups ($p=0.509$). (D) The performance pattern for distance traveled on the Barnes maze reflected the pattern shown in (C) ($p=0.033$ immediate post injury, $p=0.444$ at one month, and $p=0.165$ at 14 months). (E) During the Barnes memory probe trial when the

escape box was removed, sham and CCI groups showed similar latency to goal perimeter scores at all time points.

Figure 4. Electron transport chain activities. Complex I and COX Vmax activities were assessed in parietal cortex. (A) One-month post-injury, complex I activities were equivalent among the sham, CCI-ipsilesional, and CCI-contralesional groups. (B) COX activities were equivalent 1 month post-injury. (C) Complex I activities were equivalent 15 months post-injury. (D) COX activities were equivalent 15 months post-injury. (E) The complex I activity in the CCI-ipsilesional (injured) cortex was lower at 15 months than it was 1 month post-injury. (F) The complex I activities in the CCI-contralesional cortex were equivalent at 1 and 15 months. (G) The COX activities in the CCI-ipsilesional cortex were equivalent at 1 and 15 months. (H) The COX activities in the CCI-contralesional cortex were equivalent at 1 and 15 months.

Figure 5 Mitochondrial DNA copy number. (A) One-month post-injury the sham ipsilesional, CCI-injured ipsilesional, and CCI-injured contralesional hippocampi showed a comparable mtDNAcn. The mtDNAcn for each group increased over the subsequent 14-month aging period. At 15 months post-injury the mtDNAcn in the CCI-contralesional group exceeded that of the sham-injured and CCI ipsilesional groups. The Y axis values are mtDNAcn to nuclear DNA copy number ratios. (B) The extent of age-related mtDNAcn change, shown here as a percent increase of each 15 month measure compared to the mean group value at 1 month, was greater in the CCI-contralesional group than it was in the other two groups. (C) The trajectory of each group's mtDNAcn age-related change is depicted. Although mtDNAcn levels were comparable 1 month post-injury, 14 months later the mtDNAcn in CCI-contralesional hippocampus exceeded that in sham hippocampus ($p=0.029$ by two sample t-test) as well as that in CCI-ipsilesional hippocampus ($p=0.009$ by paired t-test). The Y axis values are mtDNAcn to nuclear DNA copy number ratios.

Figure 6. Sham-injured mouse ETC activities normalized to mtDNAcn. (A) Between 6 and 20 months of age, the mtDNAcn in the brains of the sham-injured mice increased by 42%. (B) While the complex I activity,

when referenced to total protein, did not change between 6 and 20 months of age, normalizing the complex I/protein activity from the 6 and 20-month-old mice to the corresponding 6 and 20-month-old mtDNAcn group means reveals a robust age-related difference. The Y-axis shows relative activities. (C) While the COX activity, when referenced to total protein, did not change between 6 and 20 months of age, normalizing the COX/protein activity from the 6 and 20-month-old mice to the corresponding 6 and 20-month-old mtDNAcn group means reveals a robust age-related difference. The Y-axis shows relative activities. (D) After normalizing each individual brain's complex I/protein activity to its own mtDNAcn, the mean of the values for the 20-month-old mice (n=17) was lower than it was in the 6-month-old mice (n=12). (E) After normalizing each individual brain's COX/protein activity to its own mtDNAcn, the mean of the values for the 20-month-old mice (n=17) was lower than it was in the 6-month-old mice (n=12).

Figure 7. Tg mice mtDNAcn and histopathology. (A) For the 17.5-month-old rTg4510 mice that received a TBI in young adulthood, the mtDNAcn was higher in the contralesional hippocampus than it was in the ipsilesional hippocampus ($p<0.05$ by paired t-test). (B) Frontal cortex neurofibrillary tangles revealed through thioflavin fluorescence and IF with the S396 antibody that binds phosphorylated tau. (C) For both hemispheres the number of tangle-bearing cells was greater with thioflavin than with the S396 antibody, and there were cells that were positive for one or both stains. The number of thioflavin, S396, or co-stained cells was consistently greater in the contralesional hemisphere. (D) The number of DAPI-NeuN positive cells, the number of DAPI-GFAP positive cells, the NeuN fluorescence intensity values, and the GFAP fluorescence intensity values were comparable between the ipsilesional and contralesional frontal cortices. Each parameter is expressed as a relative value of the ipsilesional cortex normalized to contralesional cortex.

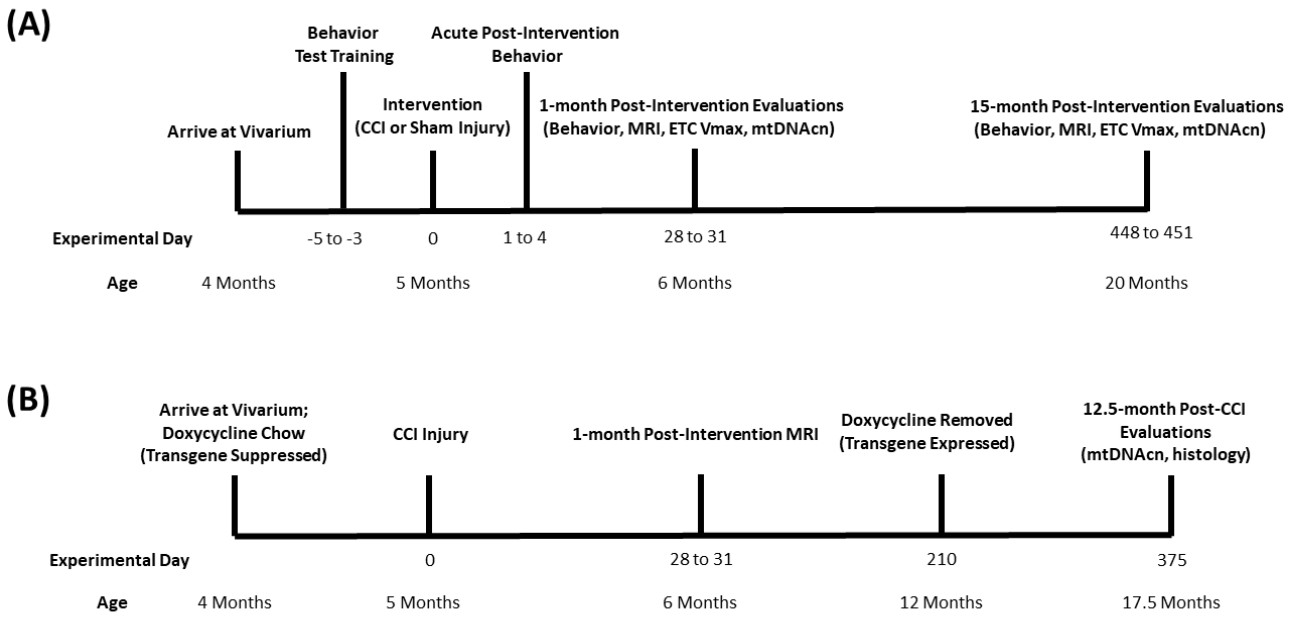
(A)
Behavior Test Training
Acute Post-Intervention Behavior
Intervention (CCI or Sham Injury)
Arrive at Vivarium
1-month Post-Intervention Evaluations (Behavior, MRI, ETC Vmax, mtDNAcn)
15-month Post-Intervention Evaluations (Behavior, MRI, ETC Vmax, mtDNAcn)
Experimental Day
-5 to -3
0
1 to 4
28 to 31
448 to 451
Age
4 Months
5 Months
6 Months
20 Months
(B)
Arrive at Vivarium; Doxycycline Chow (Transgene Suppressed)
CCI Injury
1-month Post-Intervention MRI
Doxycycline Removed (Transgene Expressed)
12.5-month Post-CCI Evaluations (mtDNAcn, histology)
Experimental Day
0
28 to 31
210
375
Age
4 Months
5 Months
6 Months
12 Months
17.5 Months

Figure 1

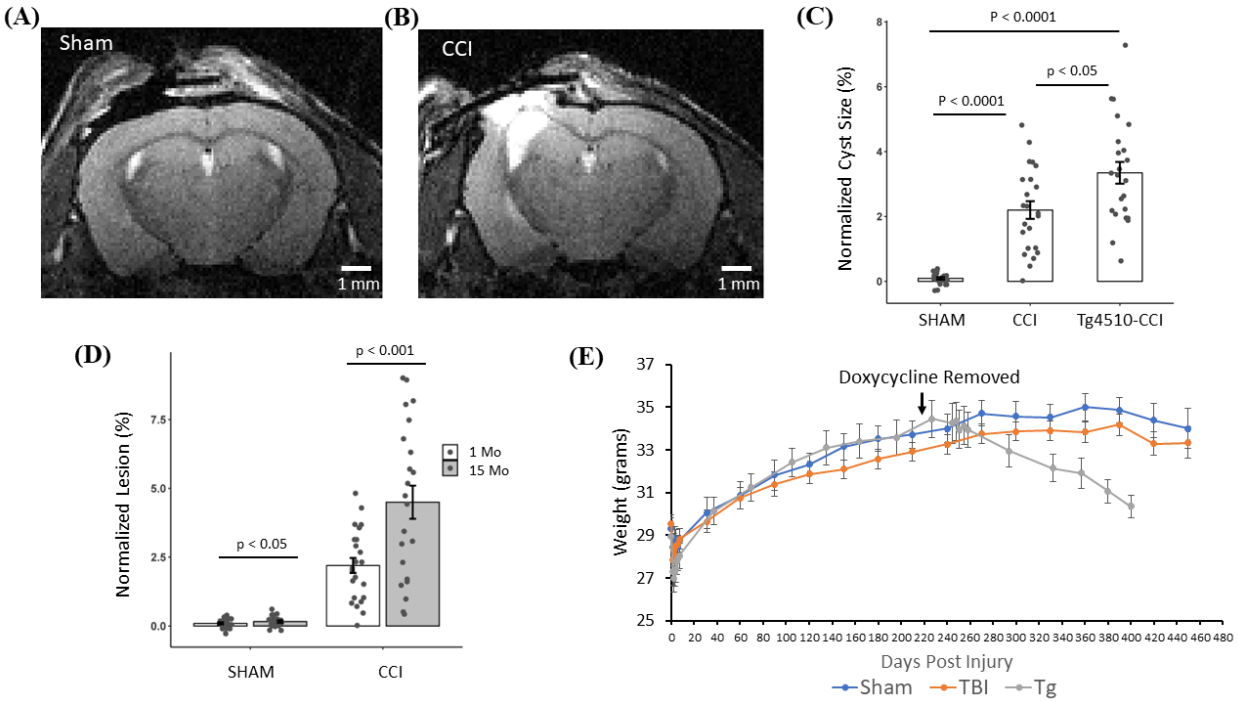
(A)
Sham
1 mm
(B)
CCI
1 mm
(C)
P < 0.0001
p < 0.05
P < 0.0001
Normalized Cyst Size (%)
SHAM
CCI
Tg4510-CCI
(D)
p < 0.001
p < 0.05
Normalized Lesion (%)
1 Mo
15 Mo
SHAM
CCI
(E)
Doxycycline Removed
Weight (grams)
Days Post Injury
Sham
TBI
Tg

Figure 2

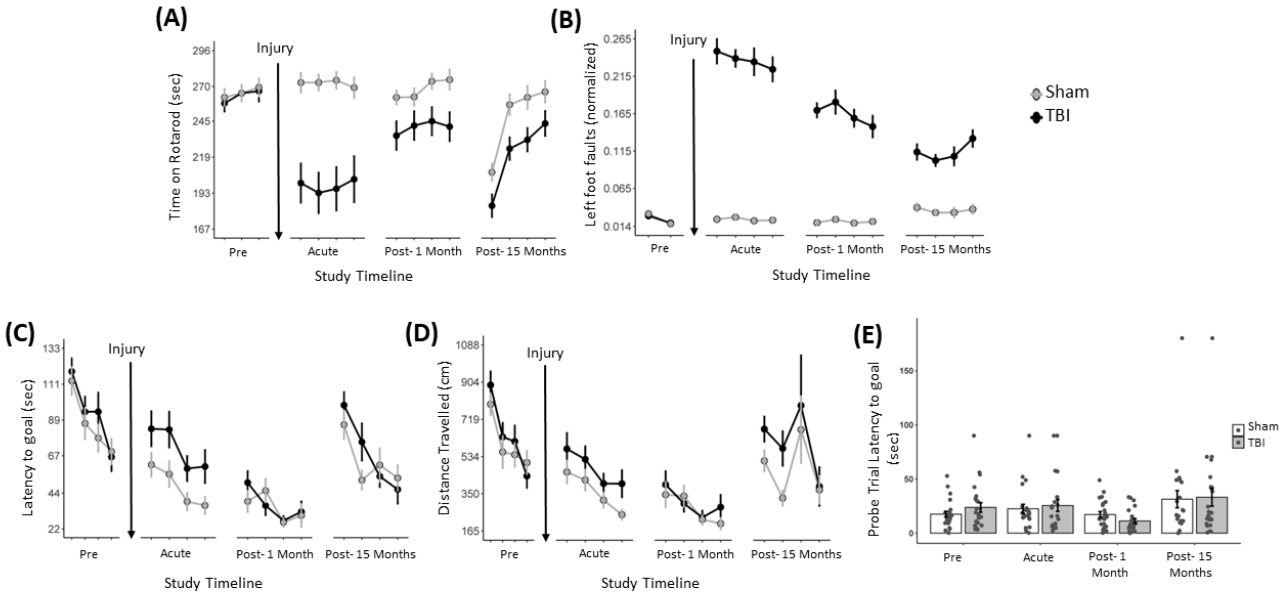
(A)
Injury
Time on Rotarod (sec)
296
270
245
219
193
167
Pre
Acute
Post- 1 Month
Post- 15 Months
Study Timeline
(B)
Injury
Left foot faults (normalized)
0.265
0.215
0.165
0.115
0.065
0.014
Pre
Acute
Post- 1 Month
Post- 15 Months
Study Timeline
Sham
TBI
(C)
Injury
Latency to goal (sec)
133
111
89
67
44
22
Pre
Acute
Post- 1 Month
Post- 15 Months
Study Timeline
(D)
Injury
Distance Travelled (cm)
1088
904
719
534
350
165
Pre
Acute
Post- 1 Month
Post- 15 Months
Study Timeline
(E)
Probe Trial Latency to goal (sec)
150
100
50
0
Pre
Acute
Post- 1 Month
Post- 15 Months
Sham
TBI

Figure 3

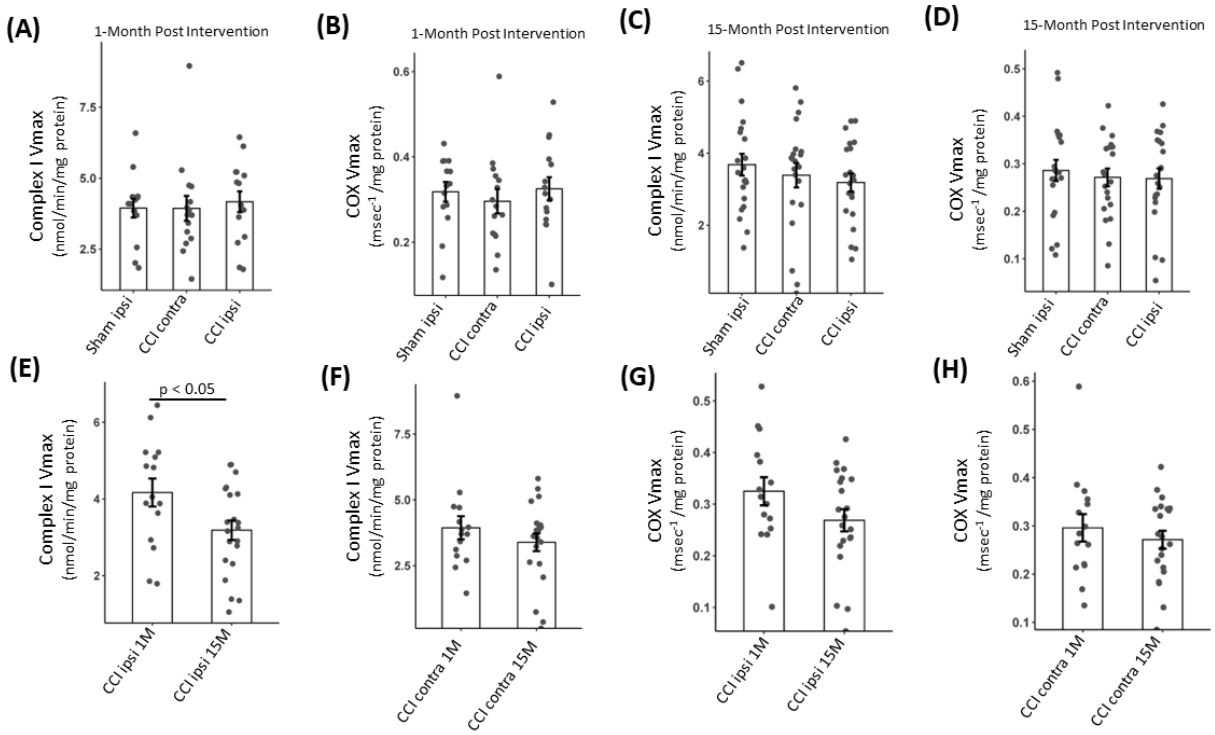
(A)
1-Month Post Intervention
Complex I Vmax
(nmol/min/mg protein)
Sham ipsi
CCI contra
CCI ipsi
(B)
1-Month Post Intervention
COX Vmax
(msec-1 /mg protein)
Sham ipsi
CCI contra
CCI ipsi
(C)
15-Month Post Intervention
Complex I Vmax
(nmol/min/mg protein)
Sham ipsi
CCI contra
CCI ipsi
(D)
15-Month Post Intervention
COX Vmax
(msec-1 /mg protein)
Sham ipsi
CCI contra
CCI ipsi
(E)
p < 0.05
Complex I Vmax
(nmol/min/mg protein)
CCI ipsi 1M
CCI ipsi 15M
(F)
Complex I Vmax
(nmol/min/mg protein)
CCI contra 1M
CCI contra 15M
(G)
COX Vmax
(msec-1 /mg protein)
CCI ipsi 1M
CCI ipsi 15M
(H)
COX Vmax
(msec-1 /mg protein)
CCI contra 1M
CCI contra 15M

Figure 4

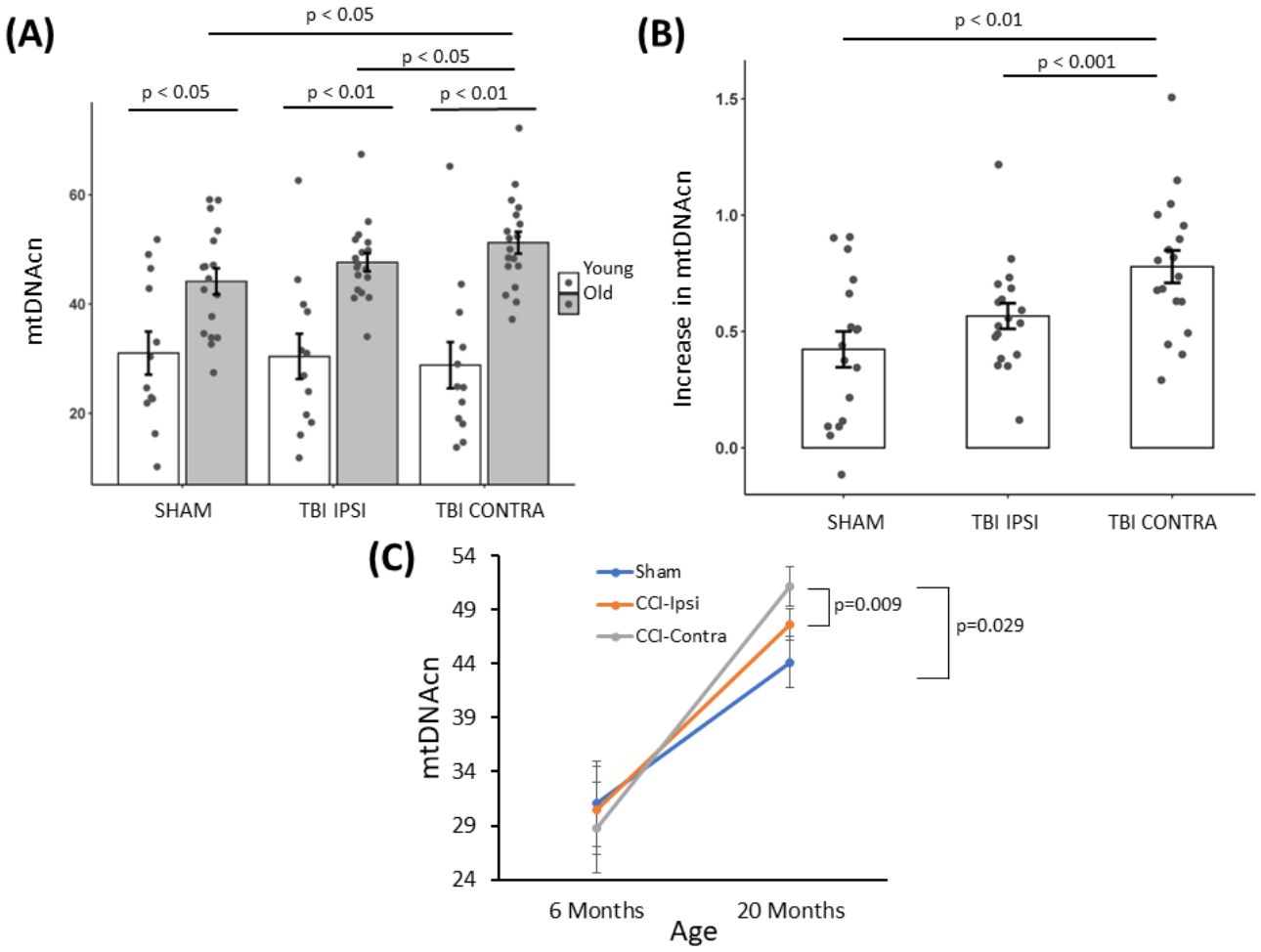
(A)
p < 0.05
p < 0.05
p < 0.05
p < 0.01
p < 0.01
mtDNAcn
60
40
20
Young
Old
SHAM
TBI IPSI
TBI CONTRA
(B)
p < 0.01
p < 0.001
Increase in mtDNAcn
1.5
1.0
0.5
0.0
SHAM
TBI IPSI
TBI CONTRA
(C)
54
49
44
39
34
29
24
mtDNAcn
Sham
CCI-Ipsi
CCI-Contra
p=0.009
p=0.029
6 Months
20 Months
Age

Figure 5

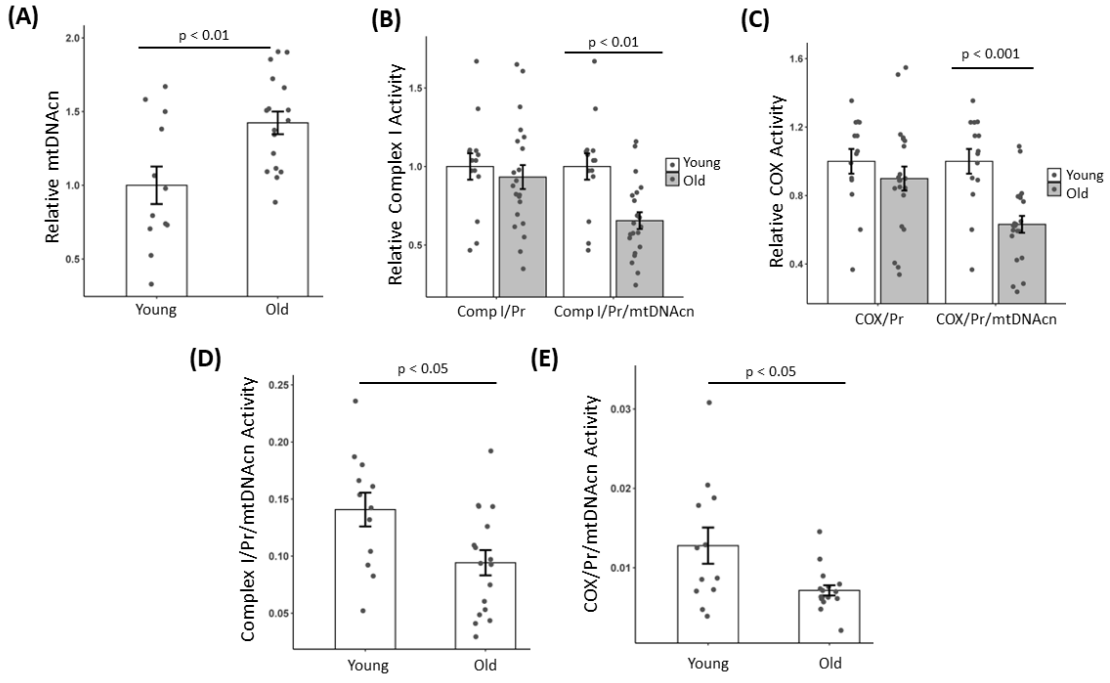
(A)
p < 0.01
Relative mtDNAcn
2.0
1.5
1.0
0.5
Young
Old
(B)
p < 0.01
Relative Complex I Activity
1.5
1.0
0.5
Young
Old
Comp I/Pr
Comp I/Pr/mtDNAcn
(C)
p < 0.001
Relative COX Activity
1.6
1.2
0.8
0.4
Young
Old
COX/Pr
COX/Pr/mtDNAcn
(D)
p < 0.05
Complex I/Pr/mtDNAcn Activity
0.25
0.20
0.15
0.10
0.05
Young
Old
(E)
p < 0.05
COX/Pr/mtDNAcn Activity
0.03
0.02
0.01
Young
Old

Figure 6

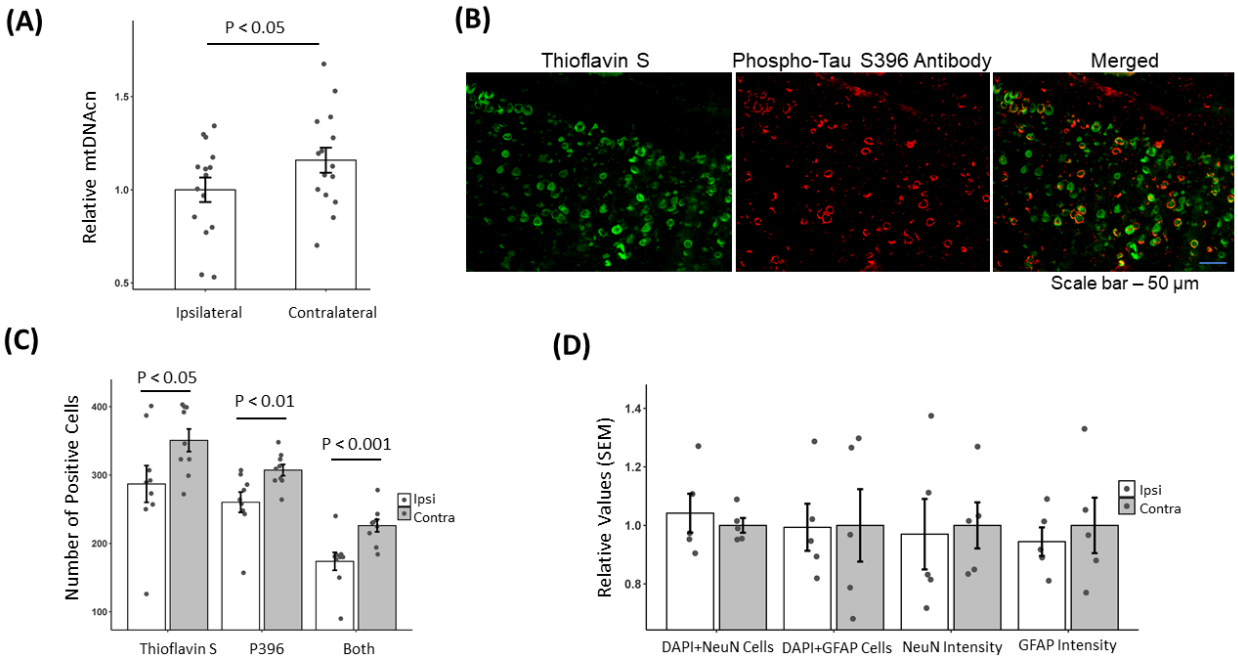
(A)
P < 0.05
Relative mtDNAcn
1.5
1.0
0.5
Ipsilateral
Contralateral
(B)
Thioflavin S
Phospho-Tau S396 Antibody
Merged
Scale bar – 50 µm
(C)
P < 0.05
P < 0.01
P < 0.001
Number of Positive Cells
400
300
200
100
Ipsi
Contra
Thioflavin S
P396
Both
(D)
Relative Values (SEM)
1.4
1.2
1.0
0.8
Ipsi
Contra
DAPI+NeuN Cells
DAPI+GFAP Cells
NeuN Intensity
GFAP Intensity

Figure 7

SUPPLEMENTARY METHODS

Histopathology

For immunofluorescence (IF) staining slides were deparaffinized and rehydrated by dipping into the following solutions: xylene, twice for 5 minutes; 100% ethanol, twice for 2 minutes; 95% ethanol, twice for 2 minutes; 70% ethanol, once for 2 minutes; 50% ethanol, once for 2 minutes; and PBS, twice for 5 minutes. Antigen retrieval was performed using a vegetable steamer. The slides were placed in a Shandon plastic spill-free slide jar (Thermo Scientific, # 3 1001362) filled with 0.01 M citrate buffer, pH 6.2, with 0.002 M EDTA. After 30 minutes in the steamer the jar was removed, and the slides were cooled for 40 minutes and washed twice for 5 minutes with PBS. Permeabilization was accomplished with 200 µl of 0.1% Triton X-100 in 0.1 M PBS, pH 7.4 for 30 minutes. The slides were placed in a glass Coplin jar and rinsed with PBS three times for 10 minutes. The washed sections were circled using a PAP pen.

Nonspecific antibody binding was blocked for 1 hour at room temperature using 10% normal donkey serum (NDS), 1% bovine serum albumin (BSA), and 0.03% Triton X-100 diluted in PBS (150 µl per section). After blocking, the slides were rinsed by dipping once in PBS. The same solution containing 1% NDS, 1% BSA, 0.03% and Triton X-100 in PBS was used for diluting the primary and secondary antibodies. Antibody incubations were performed overnight in a humidified chamber, with the sections bathed in a mix of the primary antibodies (50 µl per section) overnight at +4°C. We used the following primary antibodies: recombinant anti-tau (phospho S396) [EPR2731] ab109390 (Abcam), NeuN (E4M5P) antibody #94403 (Cell Signaling Technology), and anti-GFAP (ab4674) (Abcam). The following day the slides were washed in PBS three times, for 10 minutes each time.

A secondary antibody mix utilizing the following antibodies was prepared immediately prior to use: Donkey anti-Rabbit IgG (H+L), Alexa Fluor 647, A-31573 (Invitrogen); Donkey anti-Mouse IgG (H+L), Alexa Fluor 488, A-21202, (Invitrogen); and Donkey anti-Chicken IgY (H+L), Alexa Fluor 555, A-78949, (Invitrogen). The fluorophore-conjugated secondary antibodies were diluted at 1:300. The sections were incubated in the secondary antibody mix (150 µl per section) at room temperature for 2 hours. During all steps we minimized exposure to light. The slides were washed in PBS for 10 minutes and DAPI was applied for 10

minutes to stain nuclei. The staining procedure was completed after two 10-minute washes in PBS. The slides were then mounted with Prolong Gold antifade reagent (Invitrogen, #P36930) and sealed using clear nail polish to prevent mounting media leakage.

Thioflavin-S (#T1892, Sigma-Aldrich) staining was also performed in conjunction with tau IF with the S396 primary antibody and, in this case, Donkey anti-Rabbit IgG (H+L), Alexa Fluor 555, A-31572 (Invitrogen) as the secondary antibody. The slides were incubated in filtered 0.5% aqueous Thioflavin-S (100 ul per section, in a wet chamber, protected from light) for 7 minutes at room temperature. The slides were then washed in 3 steps: 1 minute in 70% ethanol; 6 minutes in 70% ethanol; and 3 times in distilled water, each time for 3 minutes. The washed slides were dried and mounted with Prolong Gold antifade reagent.

Images were captured using a Nikon Eclipse 90i upright fluorescent microscope. Cell counts were performed using image processing program Fiji-ImageJ (NIH, Bethesda, MD).

SUPPLEMENTARY DATA

Supplementary Figure 1. Number of mice contributing to each component of the study. (A) Thirty non-tg mice were randomized to the 1-month sham and CCI groups (15 per group). One mouse in the sham group died 2 days after the surgery and contributed no data. The other 29 mice contributed ETC data. The mtDNAcn sample sizes are smaller than the ETC sample sizes as 2-3 hippocampal samples from each group were directed towards other applications. (B) Forty-six non-tg mice were randomized to the 15-month sham and CCI groups (23 per group). Two mice in the sham group died prematurely and did not contribute ETC or mtDNAcn data. ETC and mtDNAcn data from 2 mice in the CCI group were confounded by sample transposition and the ETC and mtDNAcn data from these mice were not included. MtDNAcn data from 1 mouse in the sham group was confounded by sample transposition and not included. Forty-two mice, therefore, contributed ETC data. The mtDNAcn sample sizes are smaller than the ETC sample sizes as 3 hippocampal samples from each group were directed towards other applications. (C) Twenty-three rTg4510 transgenic mice were available at the start of the study, but 8 died before we euthanized the 15 mice that survived to 17.5 months of age (12.5 months after CCI). All 15 of those mice contributed mtDNAcn data. MRI was not conducted post-aging due to frailty. We were

able to confirm ipsilesional and contralesional anatomic landmarks for 9 of the 15 frontal cortex samples, and for that reason only 9 mice contributed to the neurofibrillary tangle analysis. Of these 9 brains, 5 had adequate tissue to enable assessments of neuron and astrocyte number.

Supplementary Figure 2. rTg4510 mouse correlational analyses. (A) For the rTg4510 mice, mtDNAcn values in the ipsilesional and contralesional hippocampi were positively correlated. (B) From the subset of rTg4510 mice we analyzed for neurofibrillary tangles, we did not observe a correlation between mtDNAcn and the number of thioflavin-stained structures in either hemisphere. (C) We did not observe a correlation between mtDNAcn and the number of P396-stained structures in either hemisphere. (D) We did not observe a correlation between mtDNAcn and the number of thioflavin-P396 stained structures in either hemisphere.

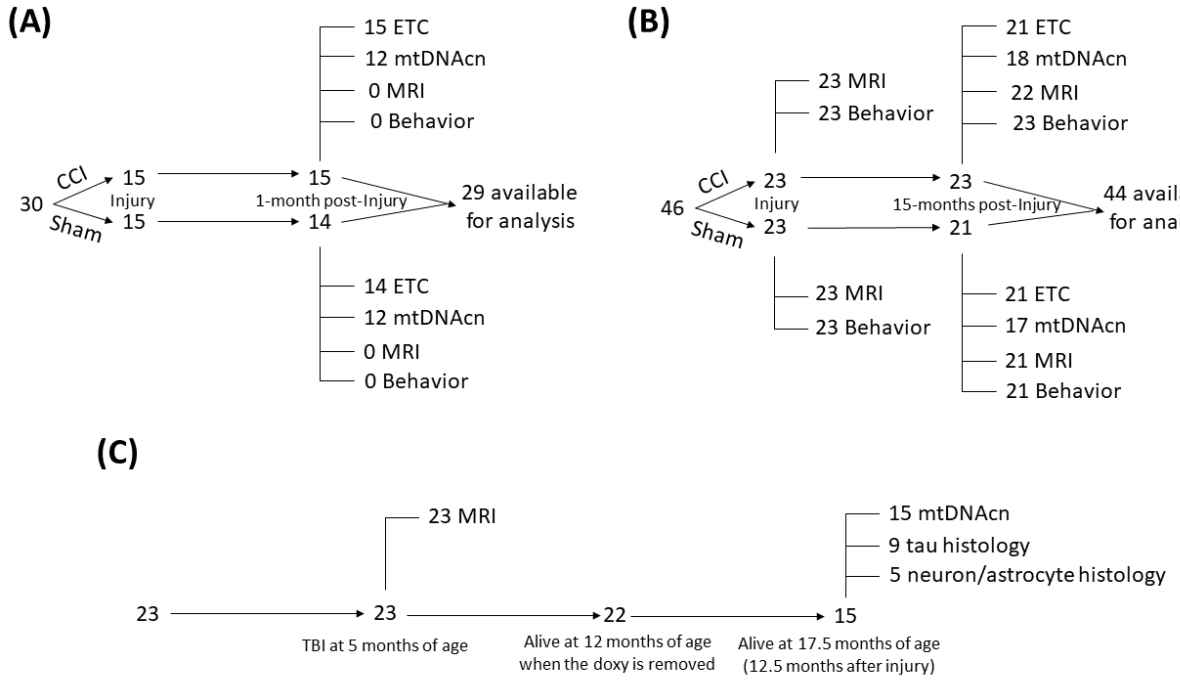

Supplementary Figure 1

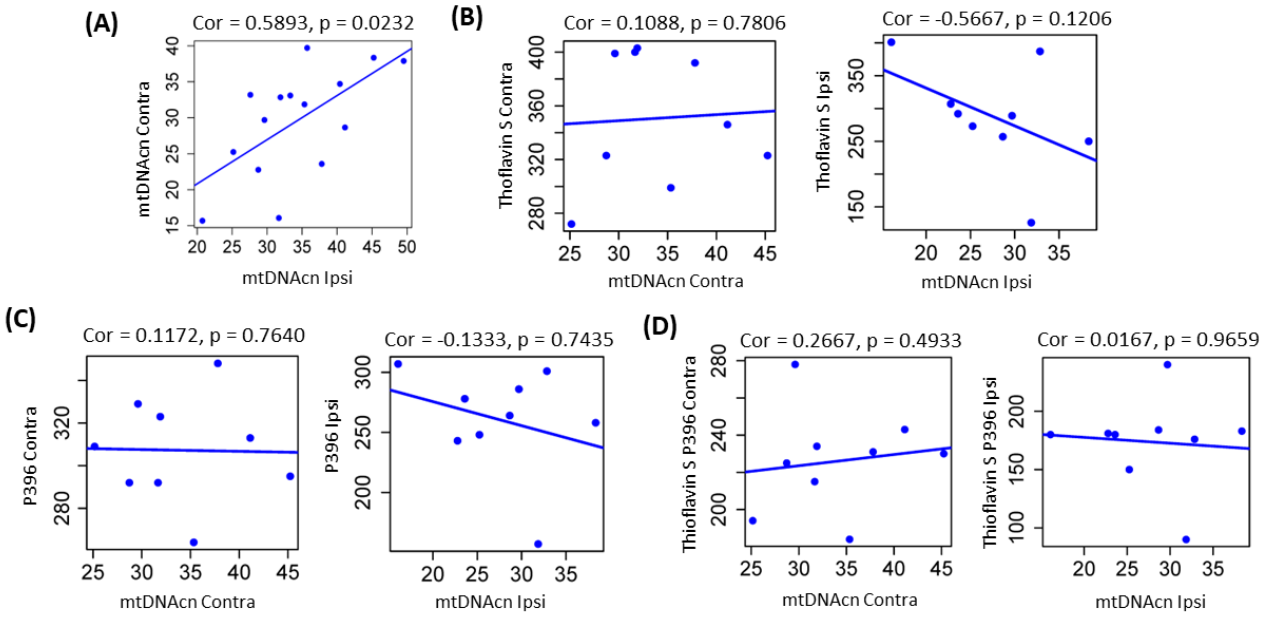

Supplementary Figure 2